



UNIVERSITÀ DEGLI STUDI DI MILANO

Scuola di Dottorato in Scienze Biologiche e Molecolari

XXV Ciclo

**PSMA-specific Antibody Fragments for Prostate Cancer**

**Imaging and Therapy**

SDD:MED16, BIO11

**Barbara Frigerio**

PhD Thesis

**Scientific tutor: Dr.ssa Mariangela Figini**

Thesis performed at Fondazione IRCCS, Istituto Nazionale per lo studio e la cura dei tumori di Milano, Dipartimento di Oncologia Sperimentale e Medicina Molecolare, Unità di Terapie Molecolari

Academic year: 2011-2012



**Contents:**

PART I .....	1
Abstract .....	3
State of art .....	4
1 The immune system .....	6
1.1 Immunoglobulin structure and functions .....	7
2 Prostate Cancer .....	13
2.1 Prostate Cancer diagnosis and standard treatment .....	14
2.2 Molecular imaging of Prostate Cancer .....	15
2.3 Immunotherapy with monoclonal antibodies .....	17
2.4 Prostate cancer immunotherapy .....	18
2.5 Target choice .....	19
3 Prostate Specific Membrane Antigen (PSMA) .....	20
4 Phage display .....	23
4.1 Phage antibody libraries .....	23
4.2 Guided selection .....	24
Aim of the project .....	26
Results and Discussion .....	28
1 ScFvD2B construction and production .....	28
2 ScFvD2B binding specificity .....	29
3 Radiolabeling .....	31
4 Competition assay .....	32
5 Stability .....	33
6 Internalization of antigen-antibody complex .....	34
7 In vivo Imaging .....	35
8 Imaging with fluorescinated antibodies .....	35
9 In vivo localization using <sup>131</sup> I – and <sup>111</sup> In-scFvD2B .....	36
Conclusion and Future Prospects .....	38
Figures .....	39
References .....	48

Acknowledgements .....	55
PART II – Published Paper .....	56
PART III .....	67
Creation of a completely human antibody fragment starting from the monoclonal antibody D2B. ....	67
Results and Discussion.....	68
1 Selection of human antibody fragments by panning with magnetic beads.	68
2 Binding of antibody fragments A and B .....	69
3 VH-A and VH-B binding .....	71
4 Mutagenesis .....	72
Conclusion and Future Prospects .....	74
Figures.....	75

**PART I**



## **Abstract**

In this study we want to evaluate the potentiality of the use of a single chain Fv (scFv) for molecular imaging and therapy of Prostate Cancer. The target of this scFv is the Prostate Specific Membrane Antigen (PSMA), a type II transmembrane protein overexpressed in advanced stages of this disease. In the past we have generated the murine antibody D2B recognizing hPSMA, whose diagnostic specificity has been investigated in xenograft murine models by imaging.

In order to obtain a smaller protein able to better penetrate the tissues we decided to convert the murine monoclonal antibody D2B into a format like scFv. This format, due to its smaller size, has also the advantage, compared to the entire antibody, to have a faster clearance from the blood.

The scFv has been constructed and its functionality has been tested with success on LNCaP cells. Using BIAcore (a technology able to measure the kinetic interaction between two molecules) we showed that the affinity of our scFv is still remarkable despite its monovalent binding.

One goal of the present study is the assessment of the potential role of this antibody fragment as diagnostic reagent for the development of radiopharmaceuticals for tumor characterization and molecular imaging. A second goal of the project is the production of a completely human antibody fragment against hPSMA in order to develop a reagent more suitable for therapy. We used phage display technology to convert the murine antibody into a human antibody applying guided selection technology which permits to generate an antibody with the specificity and functionality of the starting rodent mAb.

## State of art

Prostate Cancer (PCa), is the most common cancer in men in developed world, especially in western Europe and the Americas [Siegel *et al.* 2013] and has the highest incidence amongst male malignancies in Italy.

The number of men diagnosed with PCa remains high despite the 5-year relative survival rates have increased dramatically over the years. Since the beginning of the PSA era and the natural aging of the population, it has been observed a 25% reduction in the age-specific PCa mortality rate due to early detection screening programs but it has also been observed a dramatically increasing of the PCa worldwide incidence rate. Localized PCa is potentially curable with the use of one or a combination of modalities including brachytherapy, cryotherapy, external beam radiation therapy (RT), hormone therapy and/or radical prostatectomy (RP). However, in one-third of the patients the disease evolves into a more aggressive, metastatic and androgen-independent form (AIPCa), which fails to respond to even multi-drug treatment. Some patients with AIPCa respond to secondary hormonal manipulations. Subsequently, the disease fails to respond to further hormonal therapy and it becomes Hormone Refractory Prostate Cancer (HRPCa) [Sonpavde *et al.* 2006]. Therapy options for metastatic HRPCa remain limited. Therefore, in order to advance the treatment options for these tumors, other strategies for diagnosis and therapy are needed to improve the life expectancy of these patients.

To date, we still lack the capacity for early diagnosis and prognostic tests allowing for the evaluation of aggressiveness. Imaging is a promising diagnostic/prognostic tool and identification of sensitive and specific agents is one of the major goals for PCa. Treatments for PCa with different way of action



and minimal toxicity are greatly desired and antibody therapy could answer to these requests.

## **1 The immune system**

The immune system is the body's defense against infectious organisms and other external agents. Through a series of steps that constitute the immune response, the immune system attacks organisms and substances that invade body systems and cause disease. The immune system is made up of cells and effectors molecules responsible for two different kinds of immunity: innate immunity and adaptive immunity; their main features are compared in Table 1.1. Innate immunity (or non-specific immunity) does not require previous contact with the antigen and provides the early defense against microbes; it is created by the body's natural barriers, such as the skin, and protective substances in the mouth, the urinary tract, and on the eye surface. Another type of natural immunity is in the form of antibodies passed on from mother to child. Adaptive immunity (or specific immunity) is initiated by the specific recognition of antigens by lymphocytes; develops through exposure to specific foreign microorganisms, toxins, which are "remembered" by the body's immune system. When that antigen enters the body again, the immune system "remembers" exactly how to respond to it. Adaptive immunity is divided into humoral immunity (antibody mediated) and cell-mediated immunity.

	<i>Innate Immunity</i>	<i>Adaptive Immunity</i>
Components	<ul style="list-style-type: none"> <li>-Physical and chemical barriers</li> <li>-Phagocytic leukocytes</li> <li>-Dendritic cells</li> <li>-Natural Killer cells</li> <li>-Plasma proteins (complement)</li> </ul>	<ul style="list-style-type: none"> <li>-Humoral immunity (B cells, which mature into antibody secreting plasma cells)</li> <li>- Cell-mediated immunity (T cells which mature into effector helper and cytotoxic T cells)</li> </ul>
Activity	Always present	Normally silent
Response and potency	Immediate response, but has a limited and lower potency	Slower response (over 1-2 weeks, but is much more potent)
Specificity	General: can recognize general classes of pathogens (i.e. bacteria, viruses, fungi, parasites) but cannot make fine distinctions	Recognize highly specific antigens
Memory	No: reacts with equal potency upon repeated exposure to the same pathogen	Yes: memory cells “remember” specific pathogens; upon re-exposure to a pathogen, these cells mount a much faster and more potent second response

Tab. 1.1. Principal features of innate and adaptive immunity.

### 1.1 Immunoglobulin structure and functions

The production of antibodies or immunoglobulins (Ig) is one of the main functions of the humoral immune system.

Antibodies could be expressed on the surface of B lymphocytes or secreted from plasma cells in the circulation and tissues. The antibody molecule, represented by IgG antibodies, is a 150 kDa tetrameric molecule with a symmetric structure composed of two identical heavy (H) chains and two

identical light (L) chains joined by disulphide bonds to form a "Y" shaped molecule (Figure 1.1.1).

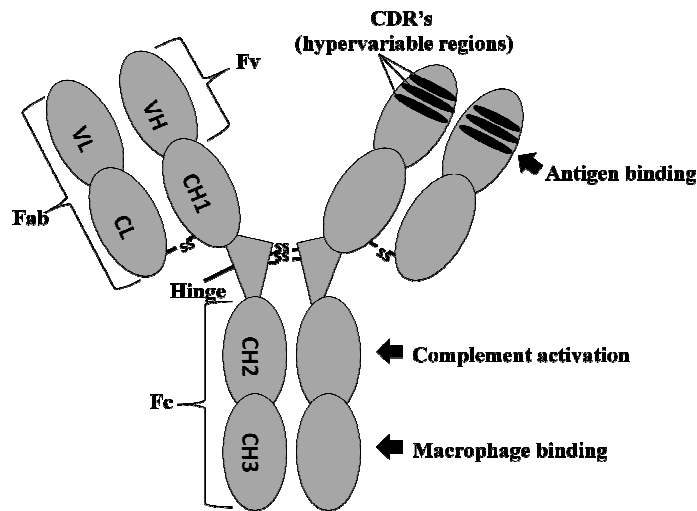


Fig. 1.1.1. Immunoglobulin G structure.

Both H and L chains consist of amino-terminal variable (V) regions, so named because they contain regions of variability in amino acid sequence, that participate in antigen recognition and carboxy-terminal constant (C) regions that mediate effector functions. The heavy chain constant domains are called CH and numbered sequentially from amino terminus to carboxyl terminus (e.g. CH1, CH2, CH3 and also CH4 for IgE and IgM). The light chain constant domain is called CL. The hinge region located between CH1 and CH2 confers flexibility to the molecule.

On the basis of differences in constant domains, antibody molecules can be divided into distinct classes, called isotypes: IgA, IgD, IgE, IgG, and IgM depending on which heavy chain they contain ( $\alpha$ ,  $\delta$ ,  $\epsilon$ ,  $\gamma$ ,  $\mu$ ). There are also two classes, or isotypes, of CL:  $\kappa$  and  $\lambda$ . In humans, about 60% of antibody molecules have  $\kappa$  light chains, and about 40% have  $\lambda$  light chains.

Each antibody molecule, containing two heavy chains and two light chains, has two identical antigen-binding sites.

In an antibody molecule, the heavy and light chain V region comprises three hypervariable regions called complementarity determining regions (CDR: CDR1, CDR2, and CDR3), responsible of the antigen-antibody binding spaced by four less variable regions called framework regions (FR: FR1, FR2, FR3, FR4), which support CDRs. Theoretically the antibody repertoire may include more than  $10^9$  different antibodies, each with unique amino acid sequences in their antigen-combining sites.

Paul Ehrlich first proposed antibody therapy in 1900 as a magic bullet, but it takes more than 100 years (1997) before the first antibody had been approved by Food and Drug Administration (FDA) for human use. At present, more than 20 antibodies are FDA approved and hundreds of new antibodies and antibody-derived reagents are in clinical trials.

We can recognize at least 4 biotechnological steps that make these results possible: Hybridoma Technology (in 1975 Köhler and Milstein), Polymerase Chain Reaction (PCR) discovery [Mullis and Faloona 1987], Transgenic Mice generation [Gordon and Ruddle 1981] and Phage Display Antibody Library [McCafferty *et al.* 1990].

The use of these technologies have allowed the conversion of existing mouse mAbs (from hybridoma technology) into mouse-human chimeric antibodies greatly refining and expanding the therapeutic potential of the modality of treatment. Chimeric antibodies are obtained by joining the antigen-binding variable domains of a mouse mAb to human constant domains. Humanized antibodies are created by grafting the antigen-binding loops, (CDRs), from a mouse mAb into a human IgG (figure 1.1.2).

Chimeric and humanized mAbs used in human clinical trials showed a variable degree of immunogenicity: chimeric mAbs in general show better pharmacokinetics and less immunogenicity than mouse mAbs but patients eventually tend to develop levels of HAMA comparable with those observed with mouse mAbs, indicating that the immunogenicity of chimeric mAbs can vary greatly in a way not yet predictable and can be directed against the mouse V region with characteristic of an anti-idiotypic response. The ideal reagent for human therapy could be a completely human antibody even if recent studies have demonstrated that many human and humanized antibodies trigger the development of anti-drug antibody responses and infusion reactions.

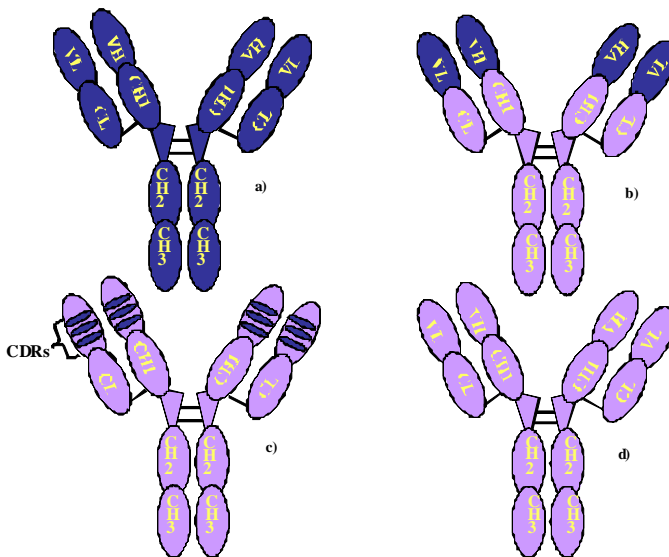


Fig. 1.1.2. Antibodies in clinical development. A) Mouse antibody; b) Chimeric antibody; c) Humanized antibody; d) Human antibody (Pictures from Frigerio et al, 2010).

The modular domain architecture of immunoglobulins has been exploited by protein engineering to create a wide variety of functional antigen-binding fragments that differ in molecular-weight (from 12 to 150 kDa) and in valency (n), from monomeric (n=1) to tetrameric (n=4) and possibly higher. The Fab format (fragment antigen binding), achievable either by proteolytic cleavage or protein engineering, contains two polypeptidic chains composed of two domains, VHCH1 and VLCL with an interchain disulfide bond at the terminal of each constant domain (molecular weight around 60 kDa). At present the most frequently used building block used to create novel antibody formats is the single-chain variable (V)-domain (scFv) consisting of a single polypeptide (30 kDa) formed by the variable regions of the heavy and light chains joined by a peptide linker of up to ~15 amino acid residues. The variable heavy and light domains can be assembled also as Fv, without a linker peptide, exploiting their natural hydrophobic interaction but this is much less stable than scFv and could not be used *in vivo*. Examples of possible antibody formats are showed in figure 1.1.3.

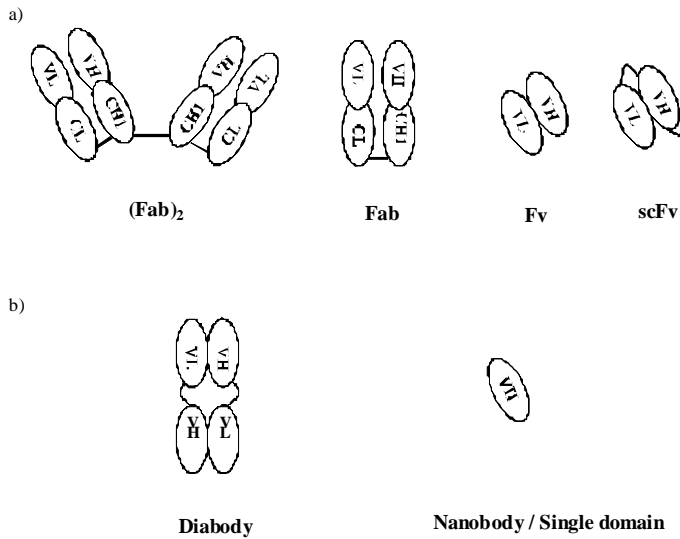


Fig. 1.1.3. Schematic representation of antibody formats (Pictures from Frigerio et al, 2010).

### 1.1.1 Nanobodies

In addition to the conventional antibodies, in the early 1990s, it was discovered that llamas, camels, dromedaries, nurse and wobbegong sharks produce antibodies composed only of heavy chains [Harmsen and de Haard 2007].

These antibodies are referred to as heavy-chain antibodies (hcAbs) and the antigen-binding site is formed only by a single domain, designated VHH in camelid and VNAR in shark and more generally, nanobody or single domain antibody (sdAb). The hcAbs have also been described in human as a pathological disorder termed “heavy chain disease” [Wahner-Roedler and Kyle 2005]. Despite the absence of light chain and their small size (15 kDa), nanobodies show a binding affinity for their cognate antigens in the range of affinities that are described for conventional antibodies.



The characteristics of nanobodies offer a number of technological advantages in the generation of engineered antibodies, as compared with conventional antibodies because are more soluble and stable than their larger counterparts. Nanobodies can get deep into tissues or cross the blood brain barrier where they have the potential to neutralize viruses or deliver toxins to cancer cells [Saerens *et al.* 2008].

Finally single-domain antibodies could be used as building blocks for novel therapeutics in a wide range of formats, including unique multivalent (multiple nanobodies with identical binding sites for the same antigen), biparatopic (two nanobodies binding two different epitopes on the same antigen), bispecific (nanobodies binding to two different antigens), bifunctional molecules [Satta *et al.* 2013] and chimeric antigen receptors (CARs) [Kloss *et al.* 2013].

## **2 Prostate Cancer**

The main function of prostate is to produce seminal fluid. Normal prostate gland is histologically divided into the stroma and the epithelium. Stroma contains the smooth muscle component of the prostate gland; the epithelium contains the glands. Glandular epithelium, which gives rise to prostate adenocarcinoma, is composed of three distinct cell types:

- secretory luminal cells: are the predominant cell type, produce prostatic secretory proteins and are androgen-dependent cells [Brawer *et al.* 1985] [Nagle *et al.* 1987] [Verhagen *et al.* 1988] [Sherwood *et al.* 1991] [Liu *et al.* 1997];
- basal cells: express androgen receptor (low level) [Brawer *et al.* 1985] [Nagle *et al.* 1987] [Verhagen *et al.* 1988] [Sherwood *et al.* 1991] [Liu *et al.* 1997] [Bui and Reiter 1998] and factors that protect from DNA damage [Bui and Reiter 1998] [De Marzo *et al.* 1998];

- neuroendocrine cells: are androgen-independent cells and seem to provide paracrine signals that support the growth of luminal cells [di Sant'Agnes 2001] [Abrahamsson 1999].

## **2.1 Prostate Cancer diagnosis and standard treatment**

At present, only biopsy (transrectal ultrasound (TRUS)-guided biopsy) from the prostate can establish the diagnosis of PCa. However, the ability of TRUS to delineate small cancer foci and differentiate between benign prostatic hyperplasia (BPH), atrophy, inflammatory processes and malignancies is limited.

Even if approximately 20% of patients are first diagnosed as having advanced carcinoma, in the great majority of cases the onset of PCa remains confined to the organ. Surgery and radiotherapy can efficiently treat organ-confined disease; however, in one-third of the patients, the disease evolves into a more aggressive, metastatic and androgen-independent form, which fails to respond to even multi-drug treatment.

In the early stages PCa grows in an androgen dependent form and the main therapeutic intervention consists of androgen ablation by pharmaco-therapeutic or surgical (orchiectomy) approaches.

Pharmacological methods for achieving androgen ablation are represented by administration of different compound: the Luteinizing-Hormone-Releasing Hormone (LHRH), the imidazole derivative ketoconazole and estrogens (such as diethylstilbestrol). The therapy is very effective in androgen-dependent cancer as a means of improving the quality of life and preventing or delaying the transition of cancer cells to AIPC<sub>a</sub> [Feldman and Feldman 2001], but these cancers eventually become androgen independent, progress and metastasize.

Food and Drug Administration (FDA) have approved four agents (Zoledronic Acid, Mitoxantrone, Docetaxel and DenosuMab) for the treatment of patients with AIPCa.

Zoledronic Acid and Mitoxantrone were approved basically as palliative, while Docetaxel is the only chemotherapeutic agent approved given a demonstrated, although modest, survival benefit [Petrylak *et al.* 2004] [Tannock *et al.* 2004]. DenosuMab is a fully human monoclonal antibody (mAb) of the IgG<sub>2</sub> subtype used for the prevention of skeletal-related events in patients with bone metastases from solid tumors. DenosuMab binds RANK ligand, preventing it from binding to the RANK receptor, and therefore inhibiting osteoclastogenesis and subsequent bone resorption [So *et al.* 2012].

Even if some patients with AIPCa respond to secondary hormonal manipulations, the disease fails to respond to further hormonal therapy and becomes HRPCa [Sonpavde *et al.* 2006].

Therapy options for HRPCa remain limited. Therefore, in order to advance the treatment options for these tumors, other strategies for diagnosis and therapy will be needed to improve the life expectancy of patients with this disease.

## **2.2 Molecular imaging of Prostate Cancer**

The conventional imaging techniques used for PCa diagnostics are ultrasound, computerized tomography (CT), radiography and magnetic resonance imaging (MRI). These techniques can offer morphologic tumor information but are less powerful for staging and disease monitoring. Consequently, newer imaging approaches able to detect pathological processes in tumor cells are used and include positron emission tomography (PET) and single photon emission computerized tomography (SPECT).

The use of radiolabeled molecular probes targeting tumor characteristics, such as increased glucose metabolism, cell proliferation or fatty acid synthesis, can provide key molecular and functional information on tumor.

Metabolic tracers are used in PCa however, their non-specificity for this disease has stimulated the development and evaluation of PCa specific molecular imaging probes. The most clinically used radiotracers are FDG, choline and FLT.

<sup>18</sup>F-fluorodeoxyglucose (FDG) is a glucose derivative and is the standard radiopharmaceutical in oncologic PET imaging. FDG internalize into the cell through specific glucose transporters (GLUTs) and is phosphorylated by hexokinase. Phosphorylated FDG cannot further undergo glycolysis and is trapped in the cells [Emonds *et al.* 2009]. Based on the Warburg effect in which the tumor cells metabolism is increased, FDG resulted a very successful tracer in clinical oncology; however results are partially disappoint in PCa patients, most likely because a low glucose metabolism is generally observed in well-differentiated PCa. Further, renal excretion, accumulation in the bladder, androgen ablation limits the diagnosis of PCa [Emonds *et al.* 2009].

Choline is a water-soluble essential nutrient that was discovered in 1864 by Adolph Strecker. Choline is the precursor for phospholipid synthesis, transmembrane signaling and lipid-cholesterol metabolism/transport. In PCa an elevation of phosphatidylcholine has been demonstrated [Ackerstaff *et al.* 2001]. Radio-labeled choline derivates, such as <sup>11</sup>C-choline, <sup>18</sup>F-fluorethyl-choline or <sup>18</sup>F-fluormethyl-choline, have been employed in several patient studies. Choline is able to detect more accurately nodal PCa spread due to a reduced renal excretion. Also, detection of primary tumors as well as restaging in patients with biochemical relapse has been performed with promising results [Rinnab *et al.* 2007]. However, Sutinen *et al.* (2004) demonstrated that the use

of  $^{11}\text{C}$ -choline is limited because is not able to distinguish PCa from hyperplasic prostate tissue.

3-Deoxy-3' - $^{18}\text{F}$ fluorothymidine ( $^{18}\text{F}$ -FLT) is a thymidine analogue used in PET imaging [Pascali *et al.* 2012]. The rate-limiting enzyme for the uptake of  $^{18}\text{F}$ -FLT is the thymidine kinase 1 (TK1). TK1 activity has been shown to be high in proliferating cells and is mainly activated in the S-phase. Despite several studies, the exact role of FLT in the imaging evaluation of response to treatment in men with PCa awaits more extensive studies. A complicating factor is also the physiologically high level of marrow FLT uptake that can hinder bone lesion detection and assessment.

### **2.3 Immunotherapy with monoclonal antibodies**

Several characteristics of PCa make it an excellent target for immunotherapy with mAbs [Bander *et al.* 2003]:

- prostate is a relatively non-essential organ;
- PCa has a very strong tendency to spread to the bone marrow and lymph nodes, locations that receive high levels of circulating antibody and have proven responsive to mAb therapies in other tumor types (e.g., lymphoma, breast cancer);
- PCa metastases are typically of small volume allowing for good antibody penetration and antigen access;
- PCa has generally a slow proliferative index, allowing ample time for an immunotherapy to induce and potentiate T-cell-mediated immunity against the tumor [Sowery *et al.* 2007].

## 2.4 Prostate cancer immunotherapy

Immunotherapy comprises both active and passive treatment approaches and could provide elimination of cancer cells without harming normal tissue and, therefore, with no or very few side effects showing great promise for improving the survival of patients.

Active immunotherapy or vaccines aim to elicit or increase tumour-reactive antibodies or lymphocytes, rather than supply these exogenously. Vaccines include injection of purified antigens, defined peptide fragments of specific antigens or the expression of antigens by viral vectors. Protein antigens and peptides must be injected together with adjuvant to improve the processing and presentation of the antigen by dendritic cells (DCs) and to provide a depot effect. Alternatively, DCs are loaded with antigen *ex vivo* prior to injection.

The term passive immunotherapy describes *ex vivo* generation of effector molecules (e.g. mAbs, cytokines), or effector cells (e.g. CD8<sup>+</sup> T cell) that are then transferred to the patient. Antibodies may: 1) block important growth factors or growth factor receptors on cancer cells or directly induce apoptosis of the cancer cell; 2) activate components of the immune system via the Fc-region of the antibody; 3) activate the antibody dependent cell-mediated cytotoxicity (ADCC) that is executed by macrophages, NK cells and probably granulocytes. In the context of PCa, the immunotherapeutic strategies are therapeutic vaccination and immune checkpoint blockade. Therapeutic vaccination include the use of PSA or PAP (prostatic acid phosphatase) using a variety of strategies such as APC (antigen presenting cells), genetically modified tumor cells, viral-based vectors, peptide and DNA [Ahmad *et al.* 2012]. Therapeutic cancer vaccination is often enhanced by the coadministration of a cytokine adjuvant such as GM-CSF (granulocyte-macrophage colony stimulating factor). Therapeutic

vaccination strategies used for PCa that seems to show some clinical promise are exemplified by sipuleucel-T and PROSTVAC-VF. Sipuleucel-T (PROVENGE, Dendreon Corp.) is an autologous vaccine prepared using patient's peripheral blood mononuclear cells (PBMC) cultured with a fusion protein consisting of PAP and GM-CSF and re-infused into the patients. PROSTVAC-VF (BN ImmunoTherapeutics) is a poxvirus-based vaccine engineered to contain PSA and 3 immune co-stimulatory molecules within a vaccinia virus or fowl pox virus vector. For PCa immune checkpoint blockade includes the use of mAb Ipilimumab for blocking CTLA-4 (anticytotoxic-T-lymphocyte associated antigen 4) and mAbs for blocking PD-1 (programmed death 1).

## 2.5 Target choice

Suitable target antigens for therapeutic antibodies are considered those molecules that are [Ross *et al.* 2005]:

- crucial to the malignant phenotype;
- not significantly expressed in vital organs and tissues;
- reproducibly measurable in clinical samples;
- well correlated with the clinical outcome.

Therefore interference or inhibition of such antigen should yields a clinical response in a significant number of patients expressing the target antigen, with minimal to absent responses in patients whose tumors do not express the target.

In addition, for drugs conjugated antibody, the target must be located on the cell surface and, when complexed with the therapeutic antibody, should internalize to facilitating tumor cell killing.

### 3 Prostate Specific Membrane Antigen (PSMA)

The PSMA gene, located on chromosome 11p [Israeli *et al.* 1994] encodes for a class II transmembrane glycoprotein [Pinto *et al.* 1996] with a NH<sub>2</sub>-terminal cytoplasmic tail of 19 amino acids, a single hydrophobic transmembrane domain of 24 amino acids, and a large extracellular domain of 707 amino acids at the COOH terminus (Figure 3.1) [Olson *et al.* 2007].

Alternative PSMA isoforms, consequence of alternative splicing of the PSMA gene, includes PSM', PSM-C and PSM-D [Schmittgen *et al.* 2003] and the newly discovered PSM-E [Cao *et al.* 2012].

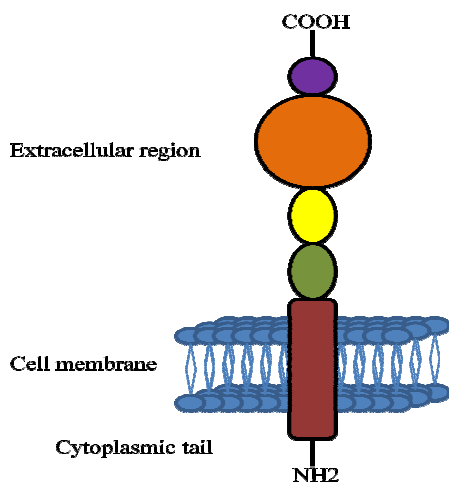


Fig. 3.1. PSMA structure.

PSMA is a carboxypeptidase with two important enzymatic functions: folate hydrolase and NAALADase (N-acetylated  $\alpha$ -linked acidic dipeptidase) and also shows an endocytotic function [Ghosh *et al.* 2005]. PSMA is expressed as a non-covalently linked homodimer with a compact three-dimensional structure on the cell surface of prostate epithelial cells [Mesters *et al.* 2006].



The enzymatic activity of PSMA is dependent on glycosylation of its extracellular domain and dimerization for proper function. Homodimerization is a fundamental feature of many transmembrane receptors. Homodimer formation is often induced by ligand binding, which is in turn necessary for mediating the cellular response of the receptor. PSMA undergoes endocytosis from the plasma membrane. This endocytosis occurs through clathrin-coated pits and involves the first five NH<sub>2</sub>-terminal amino acids of the cytoplasmic tail. Antibodies can induce PSMA internalization and the accumulation in the recycling endosomal compartment support the hypothesis that PSMA might function as a receptor internalizing a putative ligand. The capability of PSMA to internalize is a prerequisite for the delivery of cytotoxic agents.

PSMA expression has been demonstrated in normal prostate and Benign Prostate Hyperplasia (BPH), in Prostatic Intraepithelial Neoplasia (PIN) and in invasive adenocarcinoma and in the neovasculature of various non prostatic epithelial malignancies [Wright *et al.* 1995]. PSMA expression and enzymatic activity are increased in PCa: PSMA expression density increases progressively in PIN versus normal prostate epithelium, in higher grade versus lower grade carcinomas, in locally advanced versus organ confined tumours, in metastatic versus primary lesions and in hormone-independent versus hormone-dependent tumors [Wright *et al.* 1995] [Israeli *et al.* 1993] [Wright, Jr. *et al.* 1996] [Sweat *et al.* 1998].

Indeed PSMA has been correlated with aggressive disease [Rajasekaran *et al.* 2005]. In addition to its prostate gland expression, PSMA is also expressed by cells of the small intestine, proximal renal tubules, salivary glands and central nervous system, albeit at levels 100 to 1000 fold less than by prostate epithelium. The restricted expression of this molecule, which is not secreted,

has made PSMA an ideal target for anti-PSMA antibody therapy [Ghosh *et al.*2005] [Ross *et al.* 2003] [Lapidus *et al.* 2000].

7E11 was the first anti-PSMA monoclonal antibody developed and labeled with <sup>111</sup>In; the commercial name of 7E11 is ProstateScint and received Food and Drug Administration (FDA) approval in 1996 for use as a diagnostic tool for PCa [Israeli *et al.*1994]. The 7E11 mAb recognize the cytoplasmic portion of PSMA [Barren, III *et al.* 1997].

Consequently, newer generation of antibodies has been identified for therapeutic purposes based on their recognition of the extracellular domain.

The J591 mAb [Chang *et al.* 1999] directed against the extracellular domain of PSMA has been most investigated and clinical trials have been conducted with this antibody using a variety of radiolabeled and toxin conjugates. In addition, other antibodies targeting PSMA are being developed and evaluated.

As above described, PSMA has been targeted by several mAbs and some have already entered in clinical trials [Olson *et al.*2007].

Shim *et al* in 2011 demonstrated, for CD20 and HER2, that different antibodies targeting the same antigen can differ widely from one another in terms of biological, clinical characteristics and modes of action justifying our attempt to develop new anti-PSMA mAbs.

## 4 Phage display

Phage display technology consists in the selection of peptides and proteins from combinatorial libraries displayed on the surface of filamentous phage [McCafferty *et al.* 1990]. This methodology is becoming an important tool in biotechnology for the generation of diagnostic and therapeutic mAbs [Figini *et al.* 1998] and for the study of natural immune responses. A crucial advantage of this technology is the linkage of displayed antibody phenotype with its encapsulated genotype which allows the evolution of the selected binders into optimized molecules and permits the rapid determination of the aminoacidic sequence of the specific binding peptide or protein molecule by DNA sequencing of the specific insert in the phage genome (Frigerio *et al.*, 2010).

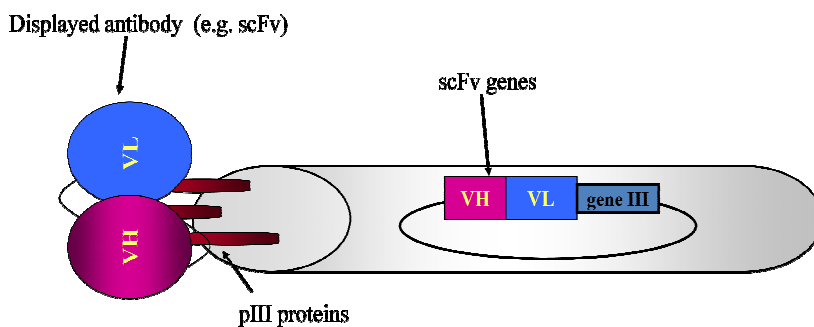


Fig. 4.1. ScFv expression on the surface of the filamentous phage (Pictures from Frigerio *et al.*, 2010).

### 4.1 Phage antibody libraries

Human antibody fragments against a variety of antigens could be isolated from diverse human antibody libraries. There are essentially three kinds of libraries: naïve, synthetic and immune. Naïve libraries are composed by antibody

variable genes isolated from healthy donors or non-immunized animals. In synthetic libraries a combinatorial diversity is created by rearranging VH and VL gene segments *in vitro* and introducing artificial CDRs of varying loop lengths using PCR and randomized primers. Immune libraries are constructed using antibody V genes obtained from immunized animals, vaccinated patients or from patients that responded to a specific disease.

## 4.2 Guided selection

Guided selection is a method for producing a human version of a rodent or any other non-human antibody. The procedure to obtain a completely human antibody (Fig.4.2.1) is performed as follows:

First step: a human VHCH phage library is used to infect *Escherichia Coli* containing the VLCL domain of the starting monoclonal antibody and production of a pool of phages expressing a different human heavy chain paired with the same murine light chain. The light chain will guide the selection of a partner human heavy chain that binds the same epitope area on the antigen as the original mouse antibody.

Second step: a) binding of phages to the immobilized target antigen b) removal of non specifically bound phages by washing c) elution of specifically bound phages d) amplification of phage library by infection and propagation of eluted phages in *Escherichia coli* e) use the new phages produced for next panning cycles. This procedure is called *panning* and allows the enrichment of those phages able to bind the immobilized target. *Panning* could be performed using immobilized antigen, antigens in solution and directly on cells or *in vivo*.

Third step: the corresponding genes of the human VHCH selected by panning are cloned into a phagemid vector containing a repertoire of human VLCL

domains. Phages expressing the same human VHCH but different human VLCL are selected as previously described.

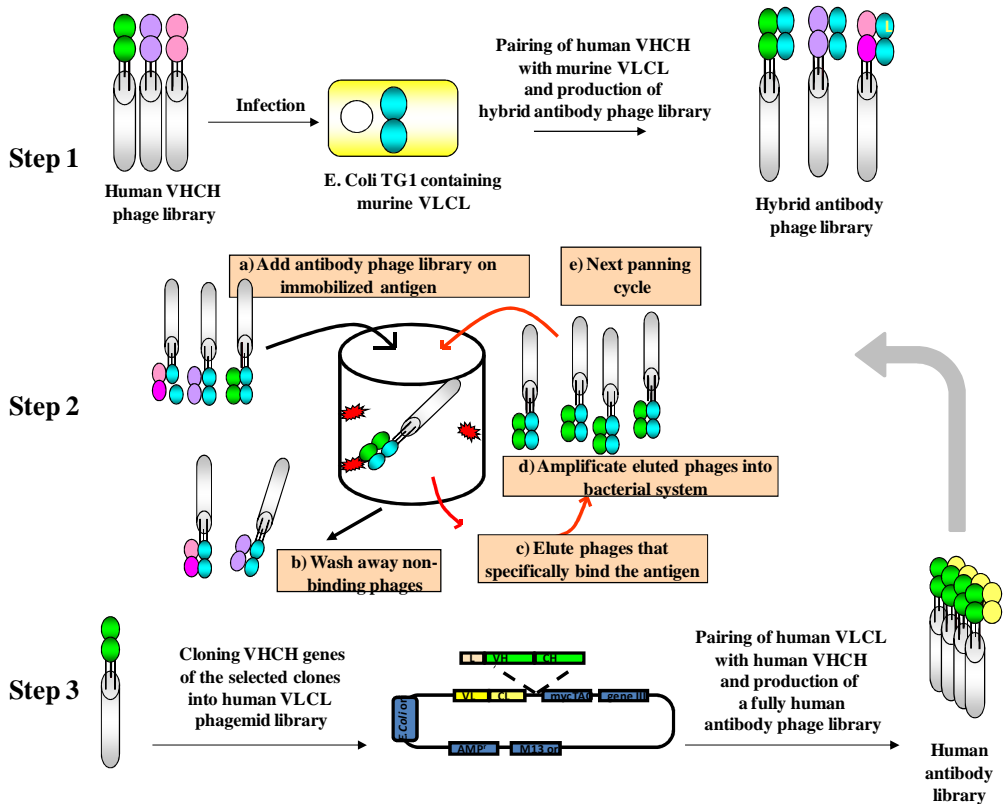


Fig. 4.2.1. Schematic representation of guided selection procedure.

The endpoint of this sequential chain shuffling procedure is a set of completely human antibodies, binding with high probability to the same epitope on the antigen as the original mouse antibody.

## **Aim of the project**

Imaging is a promising diagnostic and prognostic tool and the identification of sensitive and specific agents is one of the major goals for PCa: in this field mAbs represent ideal targeting agents. Towards this aim, PSMA, a well-known tumor associated antigen, has been targeted by several mAbs and some are currently in preclinical and clinical studies for both diagnostic and therapeutic applications [Nelson *et al.* 2010]. Overall, whole mAbs show several problems for their clinical applications. Antibody uptake by the tumor depends on a balance between favourable pharmacokinetics and efficient penetration and retention in the targeted tissue, and various characteristics of mAbs, such as molecular size, shape, affinity and valency control these properties. MAb are large molecules that are characterized by very long serum half-lives. They far exceed the renal clearance threshold (~70 kDa), preventing them from being eliminated through the kidney glomeruli. Moreover, the Fc domain of antibodies can interact with various receptors expressed at the surface of several cell types, which increase their retention in the circulation. Most importantly, the Fc portion can interact with the neonatal Fc receptor (FcRn) expressed at the surface of several cell types, including vascular endothelium cells, monocytes and macrophages as well as with barrier sites such as the blood–brain interface, the glomerular filter in the kidneys and the intestinal epithelium [Roopenian and Akilesh 2007]. ScFv fragments, due to their smaller size can more easily penetrate in solid tumor masses and the absence of the CH2-CH3 domains involved in neonatal Fc receptor binding allow a rapid clearance from the blood theoretically achieving a much greater target specificity for tumor localization [Yokota *et al.* 1992], moreover, using a

scFv fragment, the Human Anti Mouse Antibody (HAMA) response could be reduced being the Fc the most immunogenic component of the molecule.

The first aim of the project was the production and characterization of a murine scFv starting from the monoclonal antibody D2B and the following objectives were finalized:

- Conversion of the murine IgG monoclonal antibody D2B into a scFv format;
- Set up the scFv production in prokaryotic cells and verification of the stability of the reagent;
- Analysis of the specificity and affinity for PSMA expressing cells;
- Set up of the scFv radiolabelling procedures with different radioisotopes;
- *In vivo* preclinical validation of scFvD2B suitability for molecular imaging.

The second aim of the project was the creation of a completely human antibody fragment starting from the monoclonal antibody D2B using guided selection (described in Part III of this thesis).

## Results and Discussion

### 1 ScFvD2B construction and production

A new mAb directed against hPSMA antigen and named D2B (IgG1) was obtained by conventional hybridoma technology.

The cDNA obtained by reverse transcriptase of mRNA extracted from the mouse hybridoma D2B was amplified by PCR using the corresponding primers for VH and VL regions. These fragments were sequenced and showed to correspond to a VH and a VL (kappa type) regions of mouse Igs. The murine D2B use a V segment of the VK1 family (12/13 subgroup) and VH3 family. Kabat numbering was used to identify the three CDRs of the antibody [Martin 2001].

The variable regions, after re-amplification with primers for the insertion of restriction enzyme sites, were cloned into pMIMO vector and the scFv, produced in soluble form in the periplasm of bacteria cells, was purified on immobilized-metal affinity chromatography, by incubating the periplasmic extract with Ni-NTA agarose beads. The overall yield of anti-PSMA scFvD2B in *Escherichia Coli* was up to 12-14 mg/L. The size and the integrity of the purified reagent was visualized on a Coomassie-stained SDS-PAGE and detected by Western-blot with 9E10 antibody. ScFvD2B migrated as a single band of the expected molecular size of about 28 kDa.

ScFvs are relatively unstable [Cheng *et al.* 2003] and reported to form dimers and aggregates [Arndt *et al.* 1998] [Rothlisberger *et al.* 2005] following purification, particularly if they are derived from hybridoma cells [Kipriyanov *et al.* 1997]. This is due to many factors which include the presence of a disulfide bridge in the VH and VL domain, exposed hydrophobic patches at the



variable/constant domain interfaces, ionic strength, pH, linker length and at last the primary sequence, which is the most causative factor which affects the aggregation tendency [Ramm *et al.* 1999] [Nieba *et al.* 1997] [Arndt *et al.* 1998] [Pluckthun *et al.*, 1996]. Moreover the nature and strength of the VH-VL interface interactions and the type of linker used [Huston *et al.* 1991] [Raag and Whitlow 1995] [Whitlow *et al.*, 1991] increase the risk for aggregation [Arndt *et al.* 1998][Rothlisberger *et al.* 2005].

To evaluate the potential formation of dimers or aggregates, that could increase the immunogenicity of the reagent limiting its use for clinical practice, scFvD2B was analyzed by gel filtration on size-exclusion column indicating that at least 95% consisted of monomeric molecules (28 kDa) (Fig. 1). In addition, probably due to a very stable pairing of the variable chains, scFvD2B could be produced on a laboratory scale with good yield.

## **2 ScFvD2B binding specificity**

The binding specificity of scFvD2B against the antigen of interest (PSMA) in native form was verified by FACS analysis in comparison with its parent mAb using different cell lines expressing (LnCaP, PC3-hPSMA also called PC3-PIP, MCF7-hPSMA, CHO-hPSMA) or not-expressing (PC3, MCF7, CHO) PSMA. Both IgGD2B and scFvD2B showed a good and specific binding to the cell lines expressing the antigen whereas the non-related cell lines were negative (Fig. 2). ScFv binding is lower than the whole antibody as expected for a monovalent antibody fragment but shows a high binding strength demonstrated by a shift in fluorescence activity of only 1 log. Similar results were obtained when both reagents were fluorescinated or labeled with biotin followed by fluorochrome labeled avidin (data not shown) indicating also that our reagent is

suitable for a wide range of manipulations without losing its specific binding capability.

ScFvD2B used in immunohistochemistry (IHC) is able to recognize PSMA expressed on tumor surgical specimens reacting only with the tumor areas and did not stain any surrounding healthy tissue (Fig. 3A) indicating that our reagent could be suitable as diagnostic\ therapeutic agent.

BIAcore analyses, performed using as ligand soluble PSMA from lysates of LnCaP or PC3-PIP cells captured using the monoclonal antibody 7E11 specific for the intracellular domain of PSMA, showed that scFvD2B, despite its monovalency, retained a good binding strength (Fig. 3B, left panel). The lower RU observed in the sensogram with the scFv is attributable to its size, which is 6 times lower than that of the whole IgGD2B.

Based on the experimental data, association and dissociation-curves were calculated (black lines) and kinetic evaluations are summarized in Figure 3B, right panel; despite its monovalent binding, scFvD2B shows an affinity constant (KD) of 8.6 nM which is 20 times lower than that of IgGD2B, but comparable to that of the anti PSMA IgGJ591 (1.8, 3 and 15 nM in three different reports [Smith-Jones *et al.* 2000] [McDevitt *et al.* 2000] [Fracasso *et al.* 2002]), already entered in clinical use [Akhtar *et al.* 2012]. The very slow dissociation constant from the antigen argues for a high *in vivo* binding stability of scFvD2B on the PSMA. Moreover, the high affinity retained by scFvD2B indicate the possibility to use a scFv for targeting thanks to its very quick attachment to the antigen combined with a stable binding for a suitable length of time on the target and also thanks to its rapid clearance. Many studies have been performed about the importance of the best antibody formats for *in vivo* uses indicating that reducing the circulation time the affinity must be improved to obtain productive results [Leyton *et al.* 2008] [Lepin *et al.* 2010]. Our

scFvD2B with its high binding strength is promising for have a rapid localization despite a very fast clearance.

### **3 Radiolabeling**

As previous described, for protein therapeutics including mAbs, the formations of aggregates can strongly limit *in vivo* applications since they may reduce the mAb efficacy and contribute to immunogenicity. The integrity of scFvD2B after radiolabeling, evaluated by SDS PAGE (Fig. 4), was more than 99% and the formation of dimers (visualized using size-exclusion column) was less than 3% for  $^{131}\text{I}$ -scFvD2B and less than 5% for  $^{111}\text{In}$ -scFvD2B (data not shown).

All the data obtained with scFvD2B indicate that more than 95% of the reagent after radiolabeling procedure is composed of monomeric protein. This is even more important infact for this reason the purification after labelling could be avoided making possible the development of a simple labelling kit accessible to all Nuclear Medicine facilities.

After radiolabeling of scFvD2B with  $^{111}\text{In}$  and  $^{131}\text{I}$ , a radiolabeling efficacy of 96% was measured with a good radiochemical purity. The immunoreactivity of the reagents were tested on cell expressing PSMA both natural (LnCap) and ectopically expressed (PC3-PIP). No binding was observed on PC3 cells. Table 1 summarizes the efficiency of radiolabeling with  $^{111}\text{In}$  and  $^{131}\text{I}$ , the radiochemical purity, the specific activity and the immune reactivity for scFvD2B and IgGD2B.

The availability of radiolabeled reagents with high immunoreactivity allows the development of quantitative competition and internalization assays.

#### 4 Competition assay

IgGD2B and scFvD2B were analyzed for the competition capacity with other two anti-PSMA antibody commercially available: IgGJ591 (recognizing an extracellular epitope of PSMA) and IgG7E11 (recognizing an intracellular epitope of PSMA). The radiolabeled reagents (scFvD2B and IgGD2B) with competing unlabeled antibodies (scFvD2B, IgGD2B, IgG7E11 and IgGJ591) in serial dilutions are mixed in solution and added on fixed PC3-PIP cells.

After three hours of incubation and washes, the radioiodinated antibodies bound to the antigen were detected in a  $\gamma$ -counter to count the residual binding activity. The inhibiting concentration of 50% ( $IC_{50}$ ) of  $^{131}I$ -scFvD2B or  $^{131}I$ -IgGD2B binding was extrapolated from titration curves calculating the ratio between the residual binding after the competition assay and the binding of the radiolabeled antibodies alone. Unlabeled scFvD2B and IgGD2B (Fig. 5A) are able to compete with binding of  $^{131}I$ -scFvD2B on PC3-PIP cells; the mean inhibitory concentration ( $IC_{50}$ ) calculated for both unlabeled reagents was 1:1 in molar ratio. Unlabelled scFvD2B and IgGD2B compete also with radiolabeled  $^{131}I$ -IgGD2B (in similar manner of  $^{131}I$ -scFvD2B) but not with IgG7E11 and IgGJ591 (Fig. 5B).

The data obtained suggest that the binding strength of scFvD2B and IgGD2B are quite similar and that both recognize an extracellular epitope different from that recognized by IgG7E11 (as expected being an intracellular epitope) and by IgGJ591.

## 5 Stability

The scFvD2B was further analyzed to evaluate its stability in different experimental conditions. An important feature of antibodies for potential diagnostic and therapeutic applications is a sufficient resistance to serum proteases; we have evaluated its stability in mouse and human serum. The results are summarized in Fig. 7 as residual binding activity assessed by ELISA (cold reagent) or RIA (radiolabeled reagent). Incubation for 6 hours in mouse sera and for 24 hours in human sera, both potentially containing proteases, did not affect neither integrity, as assessed by SDS-PAGE (Fig. 6), nor binding activity of scFvD2B (Fig. 7). It is well known that the formations of dimers and aggregates can limit the *in vivo* applications of protein therapeutic for the reduction of mAbs efficacy and the increase of immunogenicity. For this reason the second feature analyzed is the stability of scFvD2B after long storage that could increase aggregate formation or loss of functionality. After storage for more than one year (18 months) at -20°C we observed a good maintenance of functionality (Fig. 8) and no aggregate formation, indicating a good thermostability.

The last analyzed characteristic was the stability of scFvD2B under typical conditions used for the radiolabeling of the reagent: resistance to neutral and acidic condition (i.e. HEPES 1M pH 3.5 and CH<sub>3</sub>COONa 0.4M pH4) and resistance at physiological (37°C) and high temperature (42°C, Fig. 9). ScFvD2B maintains its specific binding to cells expressing PSMA also after the exposure to physiological and harsh conditions, such as low pH (Fig. 10) and different range of temperature indicating that our reagent could be subjected to chemical manipulations without loss of binding activity.

## 6 Internalization of antigen-antibody complex

The target antigen characteristics and the fate of antigen-antibody complex after antibody binding are important features for the success of imaging and selection of therapeutic agents (radioisotopes, drugs and toxins).

PSMA-mediated antibody internalization was evaluated by epifluorescence analysis (Fig. 11A) and quantified by a radiolabel internalization assay (Fig. 11B). Both evaluations were performed at 37 °C in order to activate the internalization machinery and allow the PSMA-bound scFvD2B or IgGD2B to internalize. The same experiment was also performed at 4°C as control in order to prevent the internalization.

The internalization of the antibodies evaluated by immunofluorescence indicated that substantial amount of a surface-bond anti-PSMA scFvD2B and IgGD2B was transferred to intracellular sites at 37°C (Fig. 11A, left panel), in contrast internalization performed at 4°C (right panels) shows a reduced internalization of antibodies in the cells expressing PSMA highlighted by PSMA expression in membrane surface.

The kinetics of PSMA internalization mediated by the two reagents, radiolabeled with  $^{111}\text{In}$  (Fig. 11B), were similar; after 5 minutes at 37 °C from 20% to 60% of antigen-antibody complex was internalized and, thereafter, the amount of internalized PSMA increased over time reaching a plateau in less than 2 hours. When the internalization triggering reagent was the scFvD2B, the total amount of internalized complex was lower at each observation point but its monovalent binding was able to internalize around 40% of the bound antigen in 2 hours. Similar internalization ability was recorded when the scFvD2B was radiolabeled with  $^{131}\text{I}$  using a different chemistry of labeling (data not shown).

This observation would be consistent with the interpretation that the bivalent binding of IgGD2B crosslinking of two copies of PSMA leads to a more potent internalization than binding by a monovalent scFv. All our *in vitro* data argue for a potential *in vivo* use of scFvD2B; therefore, imaging *in vivo* experiments with both fluorescent-scFvD2B and radiolabeled-scFvD2B were performed.

## **7 *In vivo* Imaging**

Procedures involving animals and care were in conformity with institutional guidelines that comply with national and international laws and policies (D.L. 116/92 and subsequent implementing circulars).

## **8 Imaging with fluorescinated antibodies**

Mice bearing established s.c. PC3 (PSMA negative) and PC3-PIP (ectopically expressing PSMA) tumors were used for *in vivo* tumor detection capability (visualized by optical imaging) of both IgGD2B and scFvD2B labeled with a fluorochrome. The two fluorescinated reagents present different tumor detecting kinetics and biodistribution patterns (Fig. 12). IgGD2B initially showed a very diffuse signal involving both tumors while 24 hours after injection was possible to identify a specific accumulation of the antibody in PC3-PIP cells. Conversely, scFvD2B 3 hours after injection is able to show a detectable sign specific for PC3-PIP cells indicating a very high specificity. The high binding strength of scFvD2B seems to be enough to have rapid localization despite a very fast clearance usually showed for scFvs. The different tumor biodistribution of scFvD2B and IgGD2B could be explained by the fact that the IgGD2B is initial retained by Fc-receptors on many cell types in the mouse and

consequently this leads to the loss of high amount of the initial dose by non-specific binding through those receptors, which is not without systemic side effects, whereas the use of scFvD2B, lacking the Fc portion, do not have this broad and diffuse effect. By reducing the size of antibody below the filtration threshold of kidneys (70 kDa) the renal excretion is increased and therefore a decreased toxicity to this organ is expected when radioconjugated scFv are used. Moreover small size antibody fragments enabled a fast distribution into the tumor and a quick clearance from the blood and other compartments reducing also in this case the potential radiotoxic damage to healthy tissue.

These *in vivo* experimental data documented the ability of scFvD2B to specifically target only PSMA expressing PCa xenografts indicating that our reagent could be an ideal antibody fragment for the development of novel diagnostic/therapeutic methods to target imaging agents or for delivery of drugs for treatment of PSMA-positive tumors.

### **9 *In vivo* localization using $^{131}\text{I}$ – and $^{111}\text{In}$ -scFvD2B**

The choice of the radioisotopes for imaging and therapy is also important because catabolism of the radiolabeled-reagent is different.

It is known that when an antigen rapidly internalize after binding with the antibody, the complex is endocytosed and delivered to the lysosomes. Antibodies  $^{111}\text{In}$  labeled after reaching the lysosomes can be hydrolyzed to small molecular weight compounds by the resident enzymes, retained by lysosome and slowly released from the cells. On the contrary for antibodies  $^{131}\text{I}$ -labeled after degradation into the lysosomes, the low molecular weight catabolites produced are rapidly expelled from cells reducing the possible background effect created by the retention of the radioisotope.



PC3-PIP cells and PC3 cells were mixed with matrigel and the mixtures were injected subcutaneously in CD1 nude mice in the shoulder. Tumors reached dimension suitable for scintigraphy after 20 days.

$^{131}\text{I}$  – or  $^{111}\text{In}$ -scFvD2B were injected intravenously into mouse tail. Scintigraphy was performed 24 hours after injection and static images were acquired for 30 minutes.  $^{131}\text{I}$  – or  $^{111}\text{In}$ -scFvD2B biodistribution was calculated after 6 and 24 hours post injection calculating the radioactivity in tumors and representative organs.

The two radiolabeled reagents present different tumor detecting patterns.  $^{111}\text{In}$ -scFvD2B shows a very high accumulation into the kidneys, for this reason no localization of scFvD2B is detectable in scintigraphy. This data is also confirmed by the biodistribution analysis (Fig.13A) in which the kidney T/B is about 1000 cpm (at 24 hours post injection) and the tumor T/B is about 12 cpm (at 24 hours post injection). When  $^{131}\text{I}$  is used, the biodistribution analysis (Fig.13B) indicate a similar accumulation of scFvD2B in the site of the tumor and a very low background on the kidney (Fig.13B, left panel), therefore no localization were detected in mice inoculated with PC3 cells (Fig.13B, middle panel). The low background of kidneys allowed to visualize a specific localization on tumor (PC3-PIP cells) by scintigraphy (Fig.13B, right panel).

## **Conclusion and Future Prospects**

The results obtained in this thesis demonstrate that the PSMA-specific internalizing scFvD2B, due to its advantageous properties, may be an ideal antibody fragment for the development of novel diagnostic/therapeutic methods to target imaging agents or for delivery of drugs for treatment of PSMA-positive tumors.

To be able to use a scFv for targeting in humans, the reagent will be further improved in order to enter in Phase I clinical trial. ScFvD2B genes will be cloned into a specific vector (lacking the two tags: Myc-tag and His-tag normally fused to a COOH-terminal) for the expression in mammalian cells. ScFvD2B without tags will be characterized and the preclinical experiments, once radiolabeled, performed with the aim to propose it as radiolabeled diagnostic for PCa imaging and dosimetry in a Phase I clinical study.

Moreover, the high stability of the molecule argues for further exploitation of scFvD2B to generate fusion proteins and build mono-specific multimeric or bi-specific reagents that, upon preclinical validation, could hopefully enter into clinical use.

## Figures

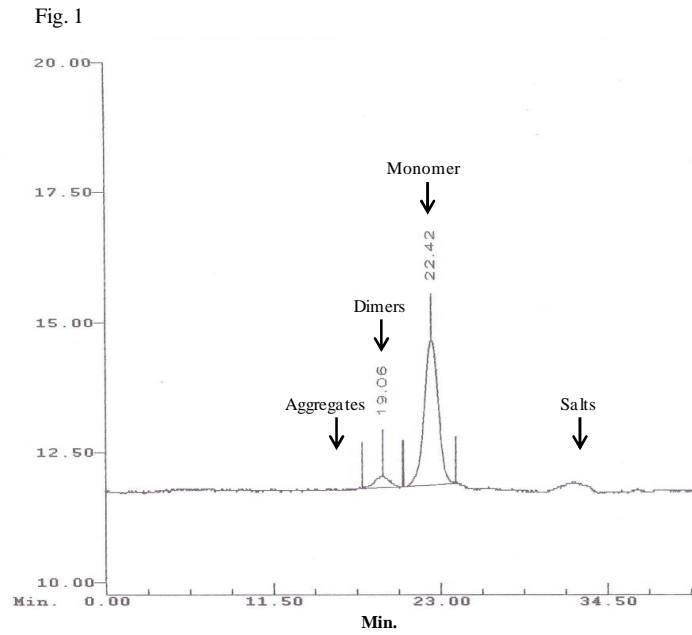


**Fig. 1.** Gel filtration on size-exclusion column. Purified scFvD2B preparation contains at least 95% of monomeric molecules (one representative experiment of 5 performed is shown).

Fig. 2

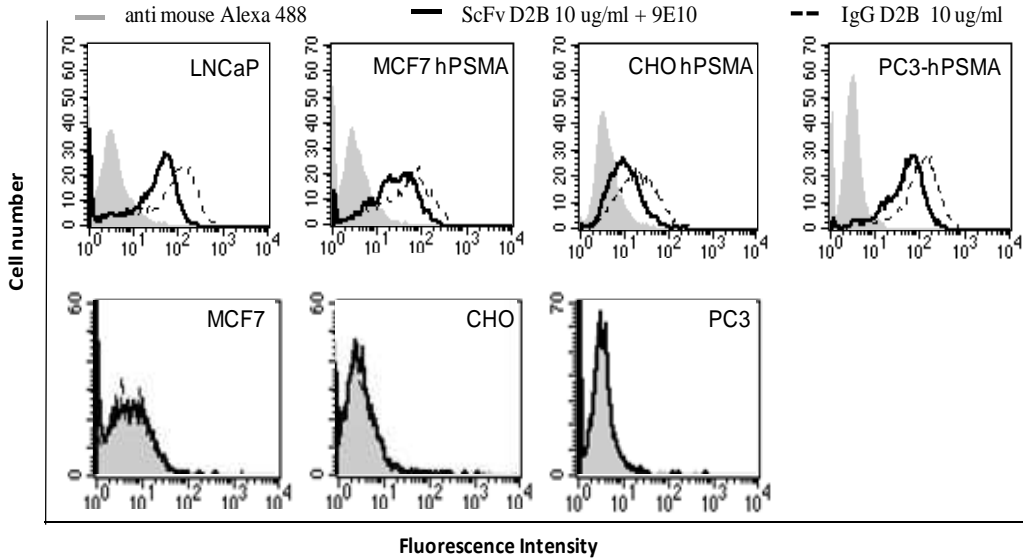


**Fig. 2.** A) FACS analysis: scFvD2B (solid line) binding in comparison to that IgGD2B (dashed line) on PSMA positive cell lines (LnCaP, MCF7-hPSMA, CHO-hPSMA and PC3-hPSMA). No binding was observed on PSMA negative cell lines (MCF7, CHO, PC3)). The shift in fluorescence was assessed relative to a negative control (gray).

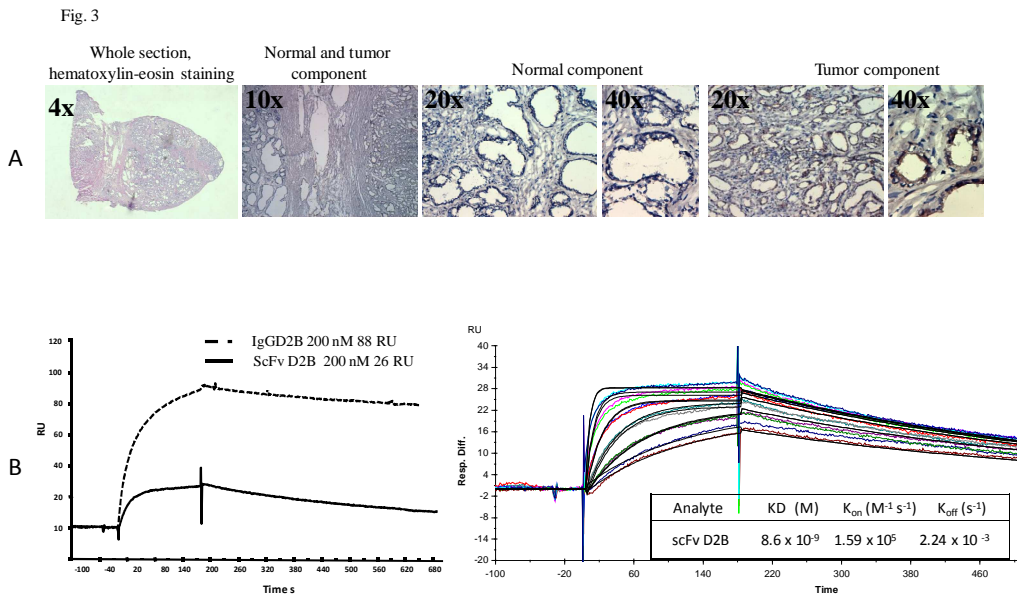


**Fig. 3.** A) IHC: ScFvD2B reactivity of prostate carcinoma. Images on serial cryostat sections from left to right: hematoxylin-eosin stained sections (4x); scFvD2B immunohistochemical stain (10x) showing no reactivity on healthy component and positive reaction on tumor component in the same section; magnification 20x and 40x of normal component; magnification 20x and 40x of tumor component. B) BIAcore analysis: (left panel) binding of scFvD2B (26RU) is only apparently lower than that observed with IgGD2B (88 RU) since its size is 6 times lower than that of the entire mAb; (right panel) Kinetic analyses of scFvD2B.

Fig. 4

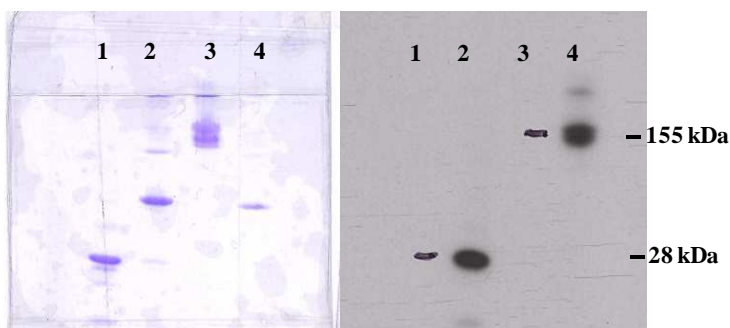


**Fig.4.** Integrity of scFvD2B before and after radiolabeling compared with IgGD2B. Left panel, SDS-PAGE loaded with cold scFvD2B (well 1) and IgGD2B (well 3) and with scFvD2B (well 2) and radiolabeled IgGD2B (well 4). Right panel, the same samples after autoradiography.

Tab. 1

Characteristics (%; mean ± SD)	<sup>131</sup> I-labeled reagents		<sup>111</sup> In-labeled reagents	
	scFvD2B (4-7 exps)	IgGD2B (2 exps)	scFvD2B (3-6exps)	IgGD2B (1 exp)
Efficiency	96.1 ± 1.4	92.0 ± 1.4	96.2 ± 0.9	99
Radiochemical Purity	99.2 ± 0.6	97.5 ± 0.7	99.2 ± 0.4	99
Specific activity	2.4 ± 0.9	1.5 ± 0.7	1.8 ± 0.8	1.9
Immunoreactivity on PSMA <sup>+</sup> cells				
LNCaP	68.0 ± 4.7	56.5 ± 2.1	52.7 ± 10.6	ND
PC3-PIP	71.3 ± 3.9	59.5 ± 2.1	63.8 ± 5.7	59
Immunoreactivity on PSMA <sup>-</sup> cells				
PC3	2.6 ± 0.9	1.9 ± 1.5	3.6 ± 1.6	1.9
A431	3.0 ± 0.2	ND	5.0 ± 1.7	ND

Tab 1. Summary of scFvD2B and IgGD2B characteristics after radiolabeling with <sup>131</sup>I and <sup>111</sup>In.

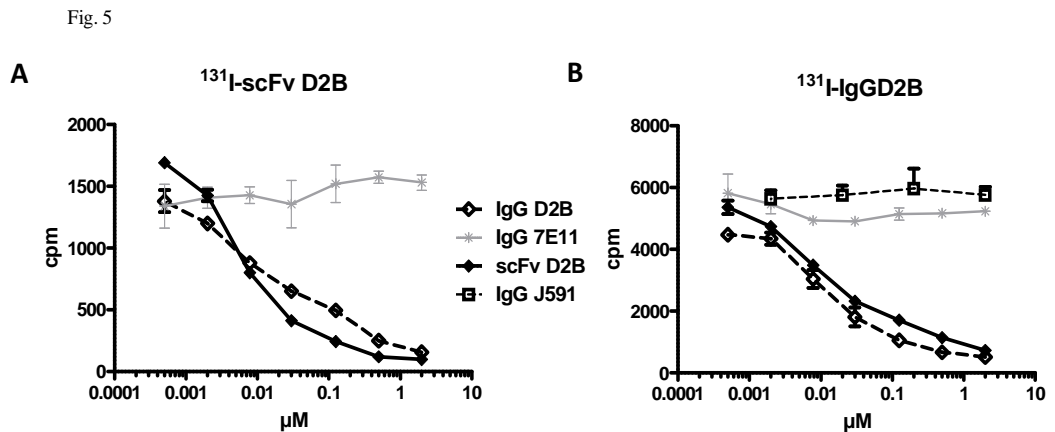
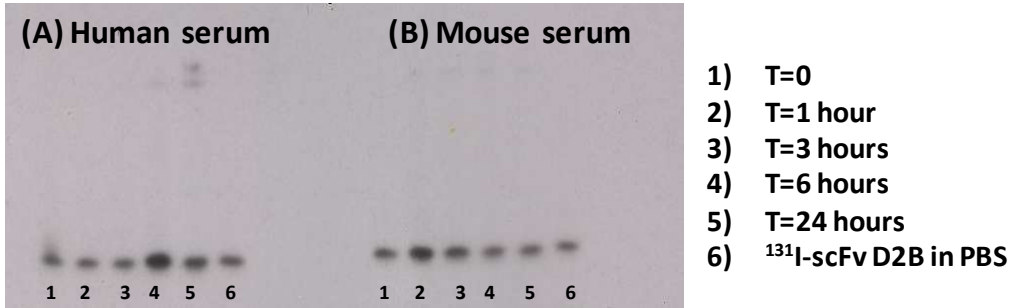


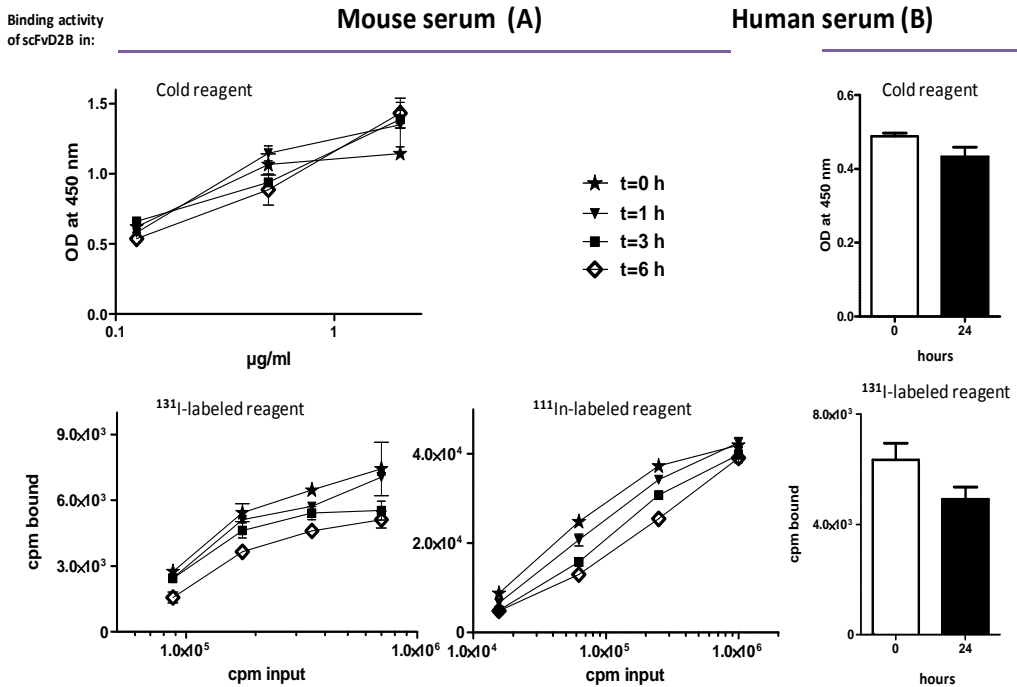
Fig. 5. Competition assay: <sup>131</sup>I-scFvD2B (A) or <sup>131</sup>I-IgGD2B (B) were mixed with titrated doses of unlabeled scFvD2B, IgGD2B, IgG7E11 or IgGJ591 and incubated on PC3-PIP cells.

Fig. 6



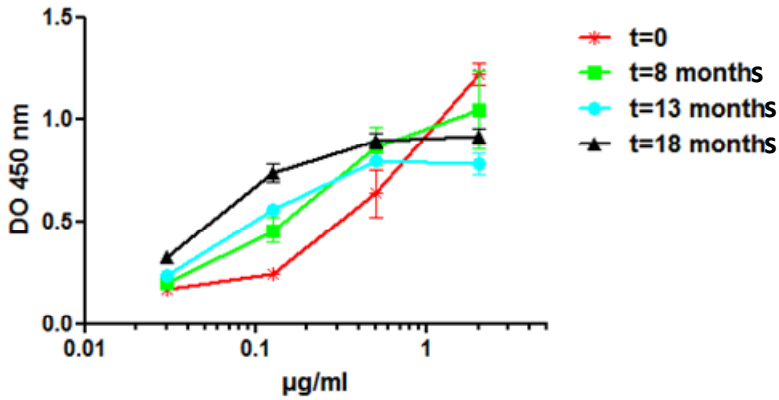
**Fig. 6.** Integrity of scFvD2B in human (A) and mouse (B) serum. SDS-PAGE Autoradiography loaded with <sup>131</sup>I-scFvD2B after mixture in human and mouse serum from t=0 to 24 hours. <sup>131</sup>I-scFvD2B diluted in PBS was added as control. The same result was obtained with <sup>111</sup>In-scFvD2B (data non shown).

Fig. 7



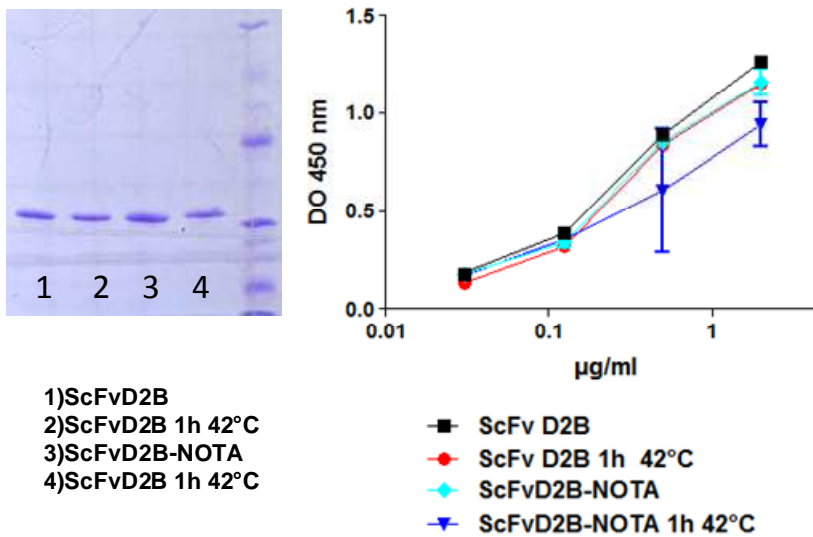
**Fig. 7.** Stability analysis. Unlabeled scFvD2B or <sup>131</sup>I / <sup>111</sup>In labelled scFvD2B stability in mouse (A) and human (B) serum at 37°C.

Fig. 8



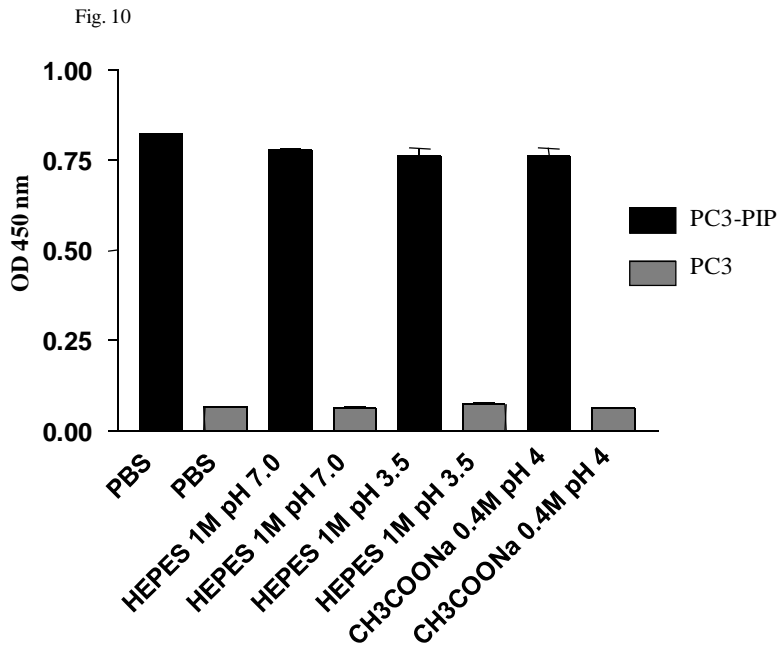
**Fig. 8.** ELISA assay. Binding on PC3-PIP cells of scFvD2B in serial dilutions after storage at -20 °C from T=0 to 18 months.

Fig. 9



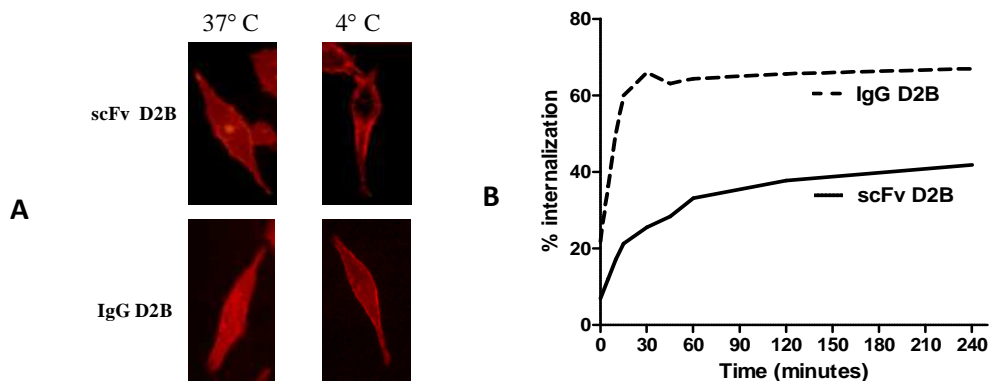
**Fig. 9.** SDS-PAGE (left panel). Integrity of scFvD2B and scFvD2B-NOTA after one hour at 42°C in comparison with non treated reagents; ELISA assay (right panel). The functionality of the same reagents was tested for binding capability in serial dilutions on PC3-PIP cells.





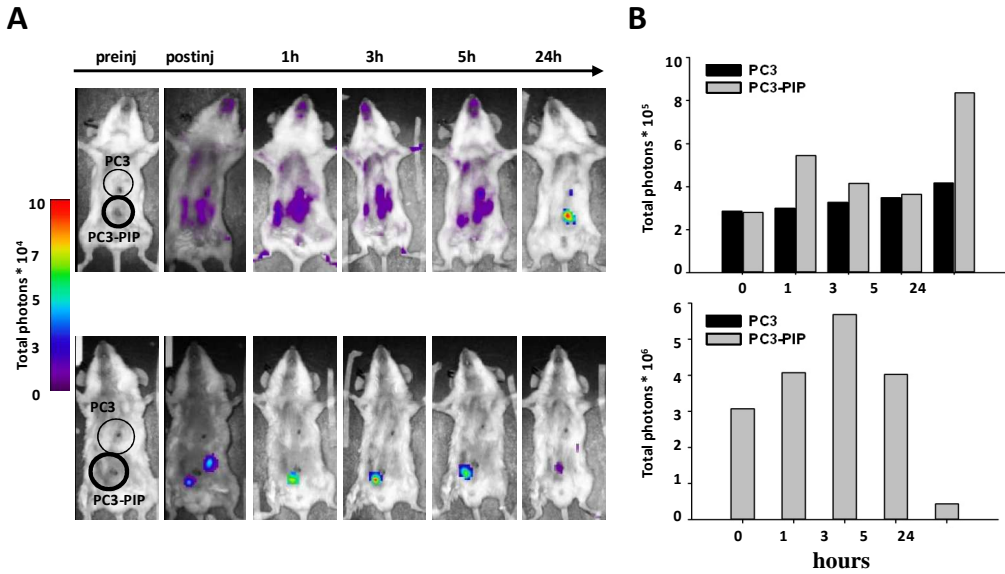
**Fig. 10.** ELISA assay. Binding of scFvD2B after exposure to low pH (scFvD2B in PBS and in HEPES pH7 were added as control).

Fig. 11



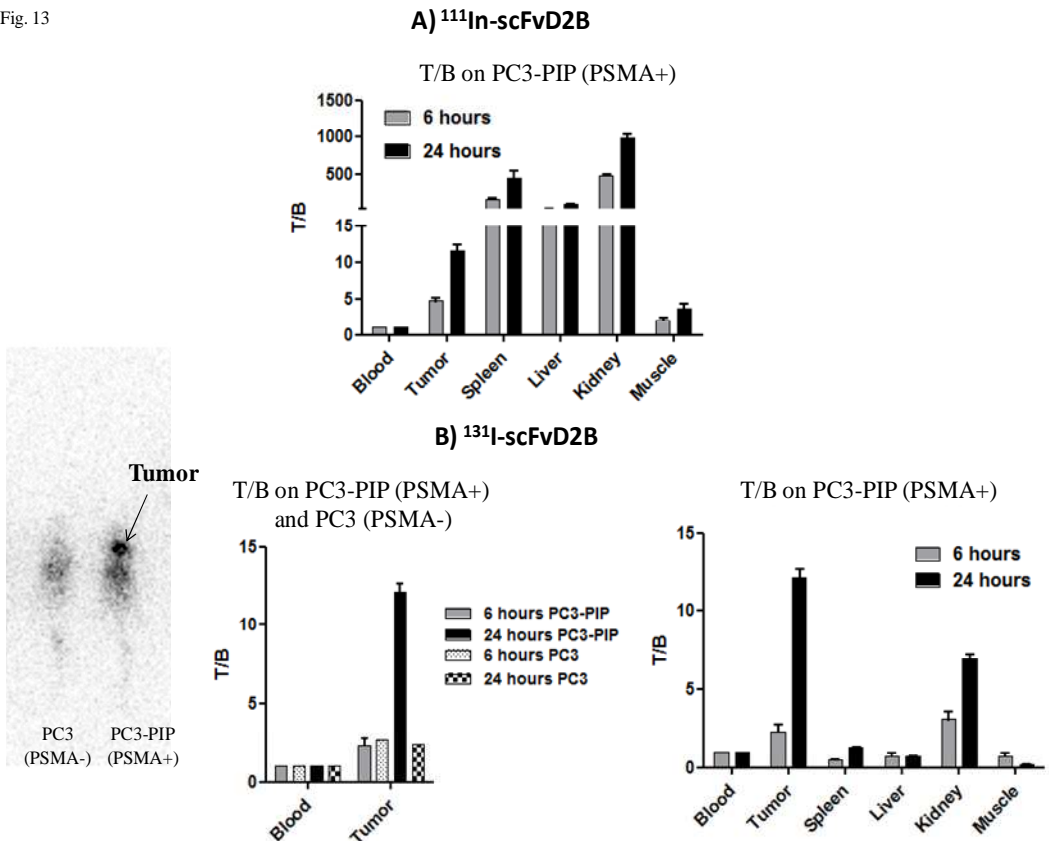
**Fig. 11.** Internalization ability of scFvD2B and IgGD2B. A) fluorescent reagents incubated at 37°C (left panel) and 4°C (right panel). B) radiolabeled scFvD2B (solid lane) and IgGD2B (dashed lane).

Fig. 12



**Fig. 12.** CYS5 ScFvD2B and IgGD2B *in vivo* biodistribution. Localization of IgGD2B (A, upper panels) or scFvD2B (A, lower panels); B) Histograms report the relative total photons emitted from regions of interest around tumor sites from mice injected with IgGD2B (upper panel) or scFvD2B (lower panel).

Fig. 13



**Fig. 13.** Radiolabeled scFvD2B *in vivo* biodistribution. A) Biodistribution of  $^{111}\text{In}$ -scFvD2B. B) Scintigraphy of  $^{131}\text{I}$ -scFvD2B (left panel); Biodistribution of  $^{131}\text{I}$ -scFvD2B on blood and tumor on PC3 and PC3-PIP cells (middle panel); Biodistribution of  $^{131}\text{I}$ -scFvD2B in all organs examined but only on PC3-PIP cell (right panel). Histograms report the relative total cpm emitted from regions of interest. (T/B: tissue/blood ratio).

## References

Abrahamsson PA. Neuroendocrine cells in tumour growth of the prostate. *Endocr Relat Cancer* 1999; 6: 503-519.

Ackerstaff E, Pflug BR, Nelson JB, Bhujwala ZM. Detection of increased choline compounds with proton nuclear magnetic resonance spectroscopy subsequent to malignant transformation of human prostatic epithelial cells. *Cancer Res* 2001; 61: 3599-3603.

Ahmad S, Sweeney P, Sullivan GC, Tangney M. DNA vaccination for prostate cancer, from preclinical to clinical trials - where we stand? *Genet Vaccines Ther* 2012; 10: 9.

Akhtar NH, Pail O, Saran A, Tyrell L, Tagawa ST. Prostate-specific membrane antigen-based therapeutics. *Adv Urol* 2012; 2012: 973820.

Arndt KM, Muller KM, Pluckthun A. Factors influencing the dimer to monomer transition of an antibody single-chain Fv fragment. *Biochemistry* 1998; 37: 12918-12926.

Bander NH, Nanus DM, Milowsky MI, Kostakoglu L, Vallabahajosula S, Goldsmith SJ. Targeted systemic therapy of prostate cancer with a monoclonal antibody to prostate-specific membrane antigen. *Semin Oncol* 2003; 30: 667-676.

Barren RJ, III, Holmes EH, Boynton AL, Misrock SL, Murphy GP. Monoclonal antibody 7E11.C5 staining of viable LNCaP cells. *Prostate* 1997; 30: 65-68.

Brawer MK, Peehl DM, Stamey TA, Bostwick DG. Keratin immunoreactivity in the benign and neoplastic human prostate. *Cancer Res* 1985; 45: 3663-3667.

Bui M, Reiter RE. Stem cell genes in androgen-independent prostate cancer. *Cancer Metastasis Rev* 1998; 17: 391-399.

Cao KY, Xu L, Zhang DM *et al.* New alternatively spliced variant of prostate-specific membrane antigen PSM-E suppresses the proliferation, migration and invasiveness of prostate cancer cells. *Int J Oncol* 2012; 40: 1977-1985.

Chang SS, Reuter VE, Heston WD, Bander NH, Grauer LS, Gaudin PB. - Five different anti-prostate-specific membrane antigen (PSMA) antibodies confirm

PSMA expression in tumor-associated neovasculature. *Cancer Res* 1999; 59: 3192-3198.

Cheng LS, Liu AP, Yang JH *et al.* Construction, expression and characterization of the engineered antibody against tumor surface antigen, p185(c-erbB-2). *Cell Res* 2003; 13: 35-48.

De Marzo AM, Meeker AK, Epstein JI, Coffey DS. Prostate stem cell compartments: expression of the cell cycle inhibitor p27Kip1 in normal, hyperplastic, and neoplastic cells. *Am J Pathol* 1998; 153: 911-919.

di Sant'Agnese PA. Neuroendocrine differentiation in prostatic carcinoma: an update on recent developments. *Ann Oncol* 2001; 12 Suppl 2: S135-S140.

Ehrlich, P. On immunity with special reference to cell life. *Proc.R. Soc.* 1900 London 66, 424

Emonds KM, Swinnen JV, Mortelmans L, Mottaghy FM. Molecular imaging of prostate cancer. *Methods* 2009; 48: 193-199.

Feldman BJ, Feldman D. The development of androgen-independent prostate cancer. *Nat Rev Cancer* 2001; 1: 34-45.

Figini M, Obici L, Mezzanzanica D *et al.* Panning phage antibody libraries on cells: isolation of human Fab fragments against ovarian carcinoma using guided selection. *Cancer Res* 1998; 58: 991-996.

Fracasso G, Bellisola G, Cingarlini S *et al.* Anti-tumor effects of toxins targeted to the prostate specific membrane antigen. *Prostate* 2002; 53: 9-23.

Frigerio B., Canevari S., Figini M. Antibody Engineering as Opportunity for Selection and Optimization of Anti- HIV Therapeutic Agents. *The Open Autoimmunity Journal*, 2010, 2, 127-138 127 1876-8946/10

Ghosh A, Wang X, Klein E, Heston WD. Novel role of prostate-specific membrane antigen in suppressing prostate cancer invasiveness. *Cancer Res* 2005; 65: 727-731.

Gordon JW, Ruddle FH. Integration and stable germ line transmission of genes injected into mouse pronuclei. *Science* 1981; 214: 1244-1246.

Harmsen MM, de Haard HJ. Properties, production, and applications of camelid single-domain antibody fragments. *Appl Microbiol Biotechnol* 2007; 77: 13-22.

Huston JS, Mudgett-Hunter M, Tai MS *et al.* Protein engineering of single-chain Fv analogs and fusion proteins. *Methods Enzymol* 1991; 203: 46-88.

Israeli RS, Powell CT, Corr JG, Fair WR, Heston WD. Expression of the prostate-specific membrane antigen. *Cancer Res* 1994; 54: 1807-1811.

Israeli RS, Powell CT, Fair WR, Heston WD. - Molecular cloning of a complementary DNA encoding a prostate-specific membrane antigen. *Cancer Res* 1993; 53: 227-230.

Jespers L, Schon O, Famm K, Winter G. Aggregation-resistant domain antibodies selected on phage by heat denaturation. *Nat Biotechnol* 2004; 22: 1161-1165.

Kipriyanov SM, Moldenhauer G, Little M. High level production of soluble single chain antibodies in small-scale *Escherichia coli* cultures. *J Immunol Methods* 1997; 200: 69-77.

Kloss CC, Condomines M, Cartellieri M, Bachmann M, Sadelain M. Combinatorial antigen recognition with balanced signaling promotes selective tumor eradication by engineered T cells. *Nat Biotechnol* 2013; 31: 71-75.

Köhler G, Milstein C. Continuous cultures of fused cells secreting antibody of predefined specificity. *Nature*. 1975 Aug 7;256(5517):495-7.

Lapidus RG, Tiffany CW, Isaacs JT, Slusher BS. Prostate-specific membrane antigen (PSMA) enzyme activity is elevated in prostate cancer cells. *Prostate* 2000; 45: 350-354.

Lepin EJ, Leyton JV, Zhou Y *et al.* An affinity matured minibody for PET imaging of prostate stem cell antigen (PSCA)-expressing tumors. *Eur J Nucl Med Mol Imaging* 2010; 37: 1529-1538.

Leyton JV, Olafsen T, Lepin EJ *et al.* Humanized radioiodinated minibody for imaging of prostate stem cell antigen-expressing tumors. *Clin Cancer Res* 2008; 14: 7488-7496.

Liu Y, Franklin RB, Costello LC. Prolactin and testosterone regulation of mitochondrial zinc in prostate epithelial cells. *Prostate* 1997; 30: 26-32.

Martin ACR. Protein Sequence and Structure Analysis of Antibody Variable Domains. In: Kontermann R, Dubel S, editors. Antibody Engineering. 2001. p. 422-39.

McCafferty J, Griffiths AD, Winter G, Chiswell DJ. Phage antibodies: Filamentous phage displaying antibody variable domains. Nature 1990; 348: 552-554.

McDevitt MR, Barendsward E, Ma D *et al.* An alpha-particle emitting antibody ([<sup>213</sup>Bi]J591) for radioimmunotherapy of prostate cancer. Cancer Res 2000; 60: 6095-6100.

Mesters JR, Barinka C, Li W *et al.* - Structure of glutamate carboxypeptidase II, a drug target in neuronal damage and prostate cancer. EMBO J 2006; 25: 1375-1384.

Mullis KB, Faloona FA. Specific synthesis of DNA in vitro via a polymerase-catalyzed chain reaction. Methods Enzymol 1987; 155: 335-350.

Nagle RB, Ahmann FR, McDaniel KM, Paquin ML, Clark VA, Celniker A. Cytokeratin characterization of human prostatic carcinoma and its derived cell lines. Cancer Res 1987; 47: 281-286.

Nelson AL, Dhimolea E, Reichert JM. Development trends for human monoclonal antibody therapeutics. Nat Rev Drug Discov 2010; 9: 767-774.

Nieba L, Honegger A, Krebber C, Pluckthun A. Disrupting the hydrophobic patches at the antibody variable/constant domain interface: improved in vivo folding and physical characterization of an engineered scFv fragment. Protein Eng 1997; 10: 435-444.

Olson WC, Heston WD, Rajasekaran AK. - Clinical trials of cancer therapies targeting prostate-specific membrane antigen. Rev Recent Clin Trials 2007; 2: 182-190.

Pascali C, Bogni A, Fugazza L *et al.* Simple preparation and purification of ethanol-free solutions of 3'-deoxy-3'-[<sup>18</sup>F]fluorothymidine by means of disposable solid-phase extraction cartridges. Nucl Med Biol 2012; 39: 540-550.

Petrylak DP, Tangen CM, Hussain MH *et al.* Docetaxel and estramustine compared with mitoxantrone and prednisone for advanced refractory prostate cancer. N Engl J Med 2004; 351: 1513-1520.

Pinto JT, Suffoletto BP, Berzin TM *et al.* Prostate-specific membrane antigen: a novel folate hydrolase in human prostatic carcinoma cells. *Clin Cancer Res* 1996; 2: 1445-1451.

Pluckthun A, Krebber A, Krebber C, Horn O, Knuper O, Wenderoth R, Nieba L, Proba K and Riesenberg D. Producing antibodies in *Escherichia coli*: from PCR to fermentation. In *Antibody engineering*, McCfferty J, Hoogenboom HR and Chiswell DJ (Eds). IRL Press, Oxford. 1996:203-252.

Raag R, Whitlow M. Single-chain Fvs. *FASEB J* 1995; 9: 73-80.

Rajasekaran AK, Anilkumar G, Christiansen JJ. Is prostate-specific membrane antigen a multifunctional protein? *Am J Physiol Cell Physiol* 2005; 288: C975-C981.

Ramm K, Gehrig P, Pluckthun A. Removal of the conserved disulfide bridges from the scFv fragment of an antibody: effects on folding kinetics and aggregation. *J Mol Biol* 1999; 290: 535-546.

Rinnab L, Mottaghy FM, Blumstein NM *et al.* Evaluation of [11C]-choline positron-emission/computed tomography in patients with increasing prostate-specific antigen levels after primary treatment for prostate cancer. *BJU Int* 2007; 100: 786-793.

Roopenian DC, Akilesh S. FcRn: the neonatal Fc receptor comes of age. *Nat Rev Immunol* 2007; 7: 715-725.

Ross JS, Gray KE, Webb IJ *et al.* Antibody-based therapeutics: focus on prostate cancer. *Cancer Metastasis Rev* 2005; 24: 521-537.

Ross JS, Sheehan CE, Fisher HA *et al.* Correlation of primary tumor prostate-specific membrane antigen expression with disease recurrence in prostate cancer. *Clin Cancer Res* 2003; 9: 6357-6362.

Rothlisberger D, Honegger A, Pluckthun A. Domain interactions in the Fab fragment: a comparative evaluation of the single-chain Fv and Fab format engineered with variable domains of different stability. *J Mol Biol* 2005; 347: 773-789.

Saerens D, Ghassabeh GH, Muyldermans S. Single-domain antibodies as building blocks for novel therapeutics. *Curr Opin Pharmacol* 2008; 8: 600-608.



Satta A, Mezzanzanica D, Turatti F, Canevari S, Figini M. Redirection of T-cell effector functions for cancer therapy: bispecific antibodies and chimeric antigen receptors. *Future Oncol* 2013; 9: 527-539.

Schmittgen TD, Teske S, Vessella RL, True LD, Zakrajsek BA. - Expression of prostate specific membrane antigen and three alternatively spliced variants of PSMA in prostate cancer patients. *Int J Cancer* 2003; 107: 323-329.

Sherwood ER, Theyer G, Steiner G, Berg LA, Kozlowski JM, Lee C. Differential expression of specific cytokeratin polypeptides in the basal and luminal epithelia of the human prostate. *Prostate* 1991; 18: 303-314.

Shim H. One target, different effects: a comparison of distinct therapeutic antibodies against the same targets. *Exp Mol Med*. 2011 Oct 31;43(10):539-49.

Siegel R, Naishadham D, Jemal A. Cancer statistics, 2013. *CA Cancer J Clin* 2013; 63: 11-30.

Smith-Jones PM, Vallabahajosula S, Goldsmith SJ *et al.* In vitro characterization of radiolabeled monoclonal antibodies specific for the extracellular domain of prostate-specific membrane antigen. *Cancer Res* 2000; 60: 5237-5243.

So A, Chin J, Fleshner N, Saad F. Management of skeletal-related events in patients with advanced prostate cancer and bone metastases: Incorporating new agents into clinical practice. *Can Urol Assoc J* 2012; 6: 465-470.

Sonpavde G, Hutson TE, Berry WR. Hormone refractory prostate cancer: Management and advances. *Cancer Treat Rev* 2006; 32: 90-100.

Sowery RD, So AI, Gleave ME. Therapeutic options in advanced prostate cancer: present and future. *Curr Urol Rep* 2007; 8: 53-59.

Sutinen E, Nurmi M, Roivainen A, Varpula M, Tolvanen T, Lehikoinen P, Minn H. Kinetics of [(11)C]choline uptake in prostate cancer: a PET study. *Eur J Nucl Med Mol Imaging*. 2004 Mar;31(3):317-24.

Sweat SD, Pacelli A, Murphy GP, Bostwick DG. Prostate-specific membrane antigen expression is greatest in prostate adenocarcinoma and lymph node metastases. *Urology* 1998; 52: 637-640.

Tannock IF, De Wit R, Berry WR *et al.* Docetaxel plus prednisone or mitoxantrone plus prednisone for advanced prostate cancer. *N Engl J Med* 2004; 351: 1502-1512.

Verhagen AP, Aalders TW, Ramaekers FC, Debruyne FM, Schalken JA. Differential expression of keratins in the basal and luminal compartments of rat prostatic epithelium during degeneration and regeneration. *Prostate* 1988; 13: 25-38.

Wahner-Roedler DL, Kyle RA. Heavy chain diseases. *Best Pract Res Clin Haematol* 2005; 18: 729-746.

Whitlow M and Filpula D: Single-chain Fv proteins and their fusion proteins. *Methods: A companion to Methods Enzymol.* 1991;2:97-105.

Wright GL, Jr., Grob BM, Haley C *et al.* Upregulation of prostate-specific membrane antigen after androgen-deprivation therapy. *Urology* 1996; 48: 326-334.

Wright GL, Haley C, Beckett ML, Schellhammer PF. Expression of Prostate-Specific Membrane Antigen in Normal, Benign, and Malignant Prostate Tissue. *Urol Oncol* 1995; 1: 18-28.

Yokota T, Milenic DE, Whitlow M, Schlom J. Rapid tumor penetration of a single-chain Fv and comparison with other immunoglobulin forms. *Cancer Res* 1992; 52: 3402-3408.

## **Acknowledgements**

I would like to express my gratitude to my PhD tutor, Dr. Mariangela Figini, for supporting me during these past years.

I am also very grateful to Dr. Silvana Canevari for her scientific helpful and suggestions.

My sincere thanks also goes to Elena for have contributed to this project always with passion and enthusiasm, and also thanks because I have had the opportunity to learn a lot working with her.

Thank to all my colleagues for the unforgettable cheerful time we shared together and in particular a special thank to Alessandro, Anna and Chiara became dear friends.

I especially thank my mom Giusy and my dad Luigi for their unconditional love and care.

I will forever be thankful to my boyfriend Emanuele for his patience and love during my good and bad times.

I big big big thank for all to my loved grandmother Tina to whom this thesis is dedicated to.

## **PART II – Published Paper**

## ARTICLE IN PRESS

European Journal of Cancer (2013) xxx, xxx–xxx

Available at [www.sciencedirect.com](http://www.sciencedirect.com)

SciVerse ScienceDirect

journal homepage: [www.ejccancer.info](http://www.ejccancer.info)

## A single-chain fragment against prostate specific membrane antigen as a tool to build theranostic reagents for prostate cancer

B. Frigerio<sup>a,1</sup>, G. Fracasso<sup>b,1</sup>, E. Luison<sup>a</sup>, S. Cingarlini<sup>c</sup>, M. Mortarino<sup>a</sup>, A. Coliva<sup>d</sup>,  
E. Seregni<sup>d</sup>, E. Bombardieri<sup>d</sup>, G. Zuccolotto<sup>e</sup>, A. Rosato<sup>e,f</sup>, M. Colombatti<sup>b</sup>,  
S. Canevari<sup>g,\*</sup>, M. Figini<sup>a,\*</sup>

<sup>a</sup> *Molecular Therapies Unit, Department of Experimental Oncology and Molecular Medicine, Fondazione IRCCS Istituto Nazionale dei Tumori, Milano, Italy*

<sup>b</sup> *Department of Pathology and Diagnostics, Section of Immunology, University of Verona, Verona, Italy*

<sup>c</sup> *Medical Oncology, Azienda Ospedaliera Universitaria Integrata (AOUI), Verona, Italy*

<sup>d</sup> *Department of Diagnostic Imaging and Radiotherapy, Fondazione IRCCS Istituto Nazionale dei Tumori, Milano, Italy*

<sup>e</sup> *Istituto Oncologico Veneto IRCCS, Padova, Italy*

<sup>f</sup> *Department of Surgery, Oncology and Gastroenterology, University of Padova, Padova, Italy*

### KEYWORDS

Prostate cancer  
Single chain Fv  
Prostate specific membrane antigen  
Imaging

**Abstract** Prostate carcinoma is the most common non-cutaneous cancer in developed countries and represents the second leading cause of death. Early stage androgen dependent prostate carcinoma responds well to conventional therapies, but relatively few treatment options exist for patients with hormone-refractory prostate cancer. One of the most suitable targets for antibody-mediated approaches is prostate specific membrane antigen (PSMA) which is a well known tumour associated antigen. PSMA is a type II integral cell-surface membrane protein that is not secreted, and its expression density and enzymatic activity are increased progressively in prostate cancer compared to normal prostate epithelium, thereby making PSMA an ideal target for monoclonal antibody imaging and therapy.

To obtain a small protein that can better penetrate tissue, we have engineered a single-chain variable fragment (scFv) starting from the variable heavy and light domains of the murine anti-PSMA monoclonal antibody D2B. scFvD2B was analysed *in vitro* for activity, stability, internalisation ability and *in vivo* for targeting specificity. Maintenance of function and immunoreactivity as well as extremely high radiolabelling efficiency and radiochemical purity were demonstrated by *in vitro* assays and under different experimental conditions. Despite its monovalent binding, scFvD2B retained a good strength of binding and was able to internalise around 40% of bound antigen. *In vivo* we showed its ability to specifically target only PSMA

\* Corresponding authors. Tel.: +39 02 2390 5151; fax: +39 02 2390 3073 (M. Figini).

E-mail address: [marianela.figini@istitutotumori.mi.it](mailto:marianela.figini@istitutotumori.mi.it) (M. Figini).

<sup>1</sup> These authors contributed equally to this work.

expressing prostate cancer xenografts. Due to these advantageous properties, scFvD2B has the potential to become a good theranostic reagent for early detection and therapy of prostate cancers.

Published by Elsevier Ltd.

## 1. Introduction

Prostate specific membrane antigen (PSMA) has generated great interest as a tumour associated molecule suitable for diagnostic and therapeutic targeting of prostate cancer since it is highly restricted to the prostate and over-expressed in all tumour stages.<sup>1–4</sup> PSMA is a transmembrane protein commonly found on the surface of late-stage and metastatic prostate cancer and is a known imaging biomarker for staging and monitoring of therapy.<sup>5</sup>

Targeted approaches have become highly investigated fields in medicine and monoclonal antibodies (mAbs) have been widely exploited on the basis of their specific recognition of tumour associated molecules. mAbs are currently in preclinical and clinical studies for both diagnostic and therapeutic applications.<sup>6</sup>

However, intact antibodies, due to their large size (155 kDa) sometimes have difficulty in penetrating tumour tissues; moreover, the presence of the constant domains allows the binding to the FcR present on many circulating cells, endothelial cells and liver cells through the CH2 and to the FcRn through the CH3 giving a prolonged half life which results in a low tumour to background ratio forcing the clinicians to perform imaging several days after the injection.

Antibody fragments could be an ideal format if the recruitment of effector functions is not necessary. A variety of approaches have been undertaken to build a functional and stable complex of the variable heavy (VH) and light (VL) domains. The commonly used single chain Fv, or 'scFv', is composed of the heavy and light chains of the antibody and utilises a flexible peptide linker to covalently join the VH and VL domains in a single polypeptide.<sup>7</sup> Unfortunately, scFvs often lack high affinity and stability, including the ability to withstand physiological concentrations of salt, pH and temperature conditions.

Herein, we characterised a scFv directed against PSMA and demonstrated that due to its intrinsic characteristics of binding strength, stability and internalisation ability, and its *in vitro* and *in vivo* targeting properties, could be successfully exploited in diagnostic and therapeutic targeted approaches.

## 2. Materials and methods

### 2.1. Cell lines and reagents

LNCaP and PC3 (human prostate cancer), MCF7 (human breast cancer) and CHO (hamster ovary) cell lines were purchased from the American Type Culture

Collection (ATCC, Manassas, MD). IGROV-1 (human ovary cancer) was provided by Dr. J. Benard and PC3-PIP, stably expressing human PSMA (hPSMA),<sup>8</sup> was provided by Dr. W. Heston. MCF7 and CHO cell lines were used to generate stable transfectants expressing hPSMA, as described.<sup>9</sup>

All cell lines were subjected to short tandem repeat (STR) analysis according to ATCC guidelines and profiles were compared to publicly available databases to verify authenticity. Total cell lysates were prepared as described.<sup>10</sup>

Hybridomas producing the mAb 7E11, directed against the intracellular domain of hPSMA (HB-10494) and the anti-myc tag mAb 9E10 (CRL-1729) were purchased from ATCC; mAb J951, directed against the extracellular domain of PSMA,<sup>11</sup> was supplied in purified form by Dr. N.H. Bander (Medical College of Cornell University, New York). The mAbs were affinity purified on protein G from culture supernatants.

### 2.2. Anti-PSMA mAb and scFv generation, purification and *in vitro* testing

The IgG1 anti-PSMA mAb, hereafter IgGD2B, was obtained by conventional hybridoma technology and affinity purified on protein A/G from culture supernatant.

Total RNA was extracted from hybridoma cells using RNeasy Total RNA Purification Kit (Qiagen). cDNA was synthesised by reverse transcription and VH and VL chains were amplified by polymerase chain reaction (PCR) using the corresponding primers (Table 1).

PCR products were cloned as a scFv (VH-linker-VL orientation) into the phagemid vector pMIMO which is a derivative of pHEN1 [10717] where the most commonly used linker (Gly<sub>4</sub>-Ser)<sub>3</sub> is added allowing the separate cloning of antibody variable domains (SFII/XHOI for VH and APALI/NOTI for VK). Electrocompetent *Escherichia coli* TG1 cells were transformed with the ligation reaction and plated on 2xTY-AGAR medium containing 100 µg/mL ampicillin. *E. coli* HB2151 cells were used for scFv soluble production as described.<sup>12</sup> Periplasmic preparations were purified by Ni-NTA agarose beads as described.<sup>13</sup>

The size, homogeneity and potential dimerisation were analysed by sodium dodecyl sulphate–polyacrylamide gel electrophoresis (SDS–PAGE), western blotting and size exclusion chromatography on a Superdex 75 HR 10/30 column (GE Healthcare). For flow cytometry refer to Fig. 2, whereas for enzyme-linked immunosorbent

## ARTICLE IN PRESS

B. Frigerio et al. / European Journal of Cancer xxx (2013) xxx–xxx

3

Table 1  
Primers used for scFvD2B cloning. Primers Mvb-3 and Mjh.f3 were used for amplification of the variable heavy (VH) region. KAP-3 and Mjklnot were used for amplification of the variable light (VL) region.

Primer	Sequence
Mvb-3	CAGGTGCAGCTGAAGSASTCAGG
Mjh.f3	TGCAGAGACAGTGACCAGAG
KAP-3	GACATTGTGATGACTCAGTCTCC
Mjklnot	GAGTCATTCTGCGGCCGCCGTTTGTATTCACAGCTTGGTGCC

assay/radioimmunoassay (ELISA/RIA), performed on LNCaP cells, see Ref. 12.

The binding of scFvD2B and IgGD2B was evaluated at 25 °C by surface plasmon resonance using a BIAcore 2000 equipped with research-grade CM5 sensor chips (Biacore AB, Uppsala, Sweden). The antibody 7E11 recognising the cytoplasmic part of PSMA was immobilised on CM5 sensor chips (Biacore AB, Uppsala, Sweden) essentially as described.<sup>14</sup> LNCaP and PC3-PIP lysates (0.5 mg/mL) or IGROV-1 lysate (0.5 mg/mL) used as non-correlated negative control, were injected three times at a flow rate of 30 µL/min for 10 min in order to enable the capture of soluble PSMA present in the lysate by 7E11 immobilised on the sensor-chip. Kinetic analyses were performed at concentrations ranging from 800 to 25 nM (all in duplicate) for 3 min at 30 µL/min and dissociation of bound analyte was allowed to proceed for 15 min without chip regeneration with glycine in order to avoid the dissociation of the soluble PSMA from 7E11. The restoring of initial baseline was verified after each injection. The data obtained were analysed by the BIAevaluation software 3.2 (global fitting) assuming a 1:1 Langmuir-binding model.

### 2.3. Immunohistochemistry

Prostate cancer samples were collected during surgical procedures from patients who gave informed consent to use excess material for investigational purposes. The immunoreactions on frozen sections were performed as described.<sup>15</sup>

### 2.4. scFvD2B and IgGD2B labelling

The following reagents were purchased: 2-(p-isothiocyanatobenzyl)-1,4,7-triazacyclononane-1,4,7-triacetic acid (Bz-NOTA, Macrocyclics, Dallas, TX, USA); human serum albumin (HSA) (25% w/v, USP) (Kedron, Castelvecchio Pascoli, Italy); ascorbic acid as a sterile and apyrogenic solution (200 mg/mL) (Bracco, Milan, Italy); high-purity grade chemicals (Sigma); <sup>125</sup>I and <sup>111</sup>In from Perkin Elmer Life and Analytical Sciences, Inc. (Boston, MA, USA), respectively. Preparation of Bz-NOTA conjugates, determination of Bz-NOTA/mAb ratio, evaluation of Bz-NOTA scFvD2B

binding and <sup>111</sup>In and <sup>131</sup>I radiolabelling were essentially as described.<sup>16,17</sup>

Binding and competitive binding studies with radiolabelled scFvD2B and IgGD2B were performed essentially as described.<sup>18</sup>

scFvD2B and IgGD2B were conjugated to Alexa 680 using the SAIVI rapid antibody labelling kit (Invitrogen, Milan, Italy) according to the manufacturer's protocol. The labelled products were purified by size exclusion chromatography on a PD10 column; protein concentration and labelling degree (fluorophore concentration extinction coefficient  $1.8 \times 10^5 \text{ M}^{-1} \text{ cm}^{-1}$ ) were determined by absorbance at 280 and 679 nm, respectively.

### 2.5. Stability analysis

scFvD2B, as an unlabelled reagent or after radiolabelling, was exposed to heat, at different pH (HEPES 1 M pH 3.5 and CH<sub>3</sub>COONa 0.4 M pH 4), human and mouse serum and residual binding activity was evaluated by ELISA/RIA after incubation at 37 °C for 6 (acid pH, mouse serum) or 24 (human serum) h.

### 2.6. In vivo imaging

*In vivo* experiments were performed using 6- to 8-week-old male Rag<sup>-/-</sup>/γc<sup>-/-</sup> mice (Charles Rivers Laboratories). Procedures involving animals and care were in conformity with institutional guidelines that comply with national and international laws and policies (D.L. 116/92 and subsequent implementing circulars). Subcutaneous tumour implants were obtained by injecting  $1 \times 10^6$  PC3 or PC3-PIP cells at two different sites in the same animals. When tumours were palpable (about 3–4 mm in diameter), fluorophore-labelled IgGD2B (50 µg) or scFvD2B (80 µg) were injected i.v., and imaging was performed by total body scanning at different time points using an MX2 apparatus (ART, Montreal, QC, Canada), as previously reported.<sup>19</sup>

### 2.7. Statistical analysis

The results of ELISA/RIA and internalisation assays are indicated as mean ± SD. Significance levels were estimated by Student's *t*-test and a *P* value <0.05 was considered significant. Calculations were done using GraphPad Prism software.



### 3. Results

#### 3.1. scFv construction and binding specificity

The cDNA from IgGD2B was amplified using the primers reported in Table 1 and sequenced; D2B uses a V segment of the VK1 family (12/13 subgroup) and a VH belonging to the VH3 family. Kabat numbering was used to identify the three CDRs of the heavy and light chain variable regions.<sup>20</sup>

The overall yield of anti-PSMA scFvD2B in *E. coli* was up to 12–14 mg/L. The purified scFv, as visualised on a Coomassie-stained SDS–PAGE, detected on a Western-blot with 9E10 or evaluated by size exclusion chromatography, consisted mainly of monomeric molecules (28 kDa) with no aggregates and only 5–8% of dimers (Fig. 1).

The binding specificity of scFvD2B was verified by flow cytometry in comparison to IgGD2B in cell lines expressing (LnCaP, PC3-PIP, MCF7-hPSMA, CHO-hPSMA) or not-expressing (PC3, MCF7, CHO) hPSMA. Both reagents showed good and specific binding (Fig. 2A). Similar results were obtained with both anti-PSMA reagents directly labelled with fluorescein or biotin followed by fluorochrome labelled avidin (data not shown). When assessed by immunohistochemistry (IHC) for ability to recognise PSMA expressed on tumour surgical specimens, scFvD2B stained only the tumour areas and not the surrounding healthy tissue (Fig. 2B).

BIAcore analysis was performed using, as ligand, soluble PSMA from LnCaP or PC3-PIP lysates captured by 7E11 mAb recognising an intracellular epitope. The binding between 7E11 and PSMA did not interfere with that of D2B and was very stable allowing further analyses on the complex. The antibody fragment, despite its monovalent binding, retained good binding strength (Fig. 2C, panel a). Based on experimental data, association and

dissociation-curves were calculated and kinetic evaluations (summarised in Fig. 2C, panel b) gave rise to a calculated affinity constant (KD) of 8.6 nM for scFvD2B.

#### 3.2. Radiolabelling, competition and stability

The unusually high radiolabelling efficiency and radiochemical purity (>95%), specific activity and maintenance of immunoreactivity of both <sup>131</sup>I- and <sup>111</sup>In-scFvD2B and -IgGD2B are summarised in Table 2. After radiolabelling, the integrity of scFvD2B (visualised by SDS–PAGE, Fig. 3C) was more than 99% and the presence of dimers (by size exclusion chromatography) did not increase. Determination of scFvD2B epitope specificity was performed using a competitive assay in which the antigen is immobilised, and a mixture of radiolabelled scFvD2B or IgGD2B with competing unlabelled antibodies (scFvD2B, IgGD2B, IgG7E11 and IgGJ591) was tested for residual binding activity.

Both unlabelled scFvD2B and IgGD2B (Fig. 3A) competed with binding of radiolabelled <sup>131</sup>I-scFvD2B to PC3-PIP cells; the mean inhibitory concentration (IC<sub>50</sub>) of scFvD2B and IgG2B was 10 and 19.6 nM, respectively. Similarly both unlabelled scFvD2B and IgGD2B competed with radiolabelled <sup>131</sup>I-IgGD2B while the other two anti-PSMA mAbs 7E11 and J591 did not compete (Fig. 3B). In these experimental conditions the IC<sub>50</sub> of scFvD2B and IgG2B was 18 and 11 nM, respectively. Since the labelled reagents were tested at 20 nM, these data indicate that the binding strength of the two anti-PSMA reagents is quite similar inhibiting 50% of labelled reagents at roughly an equimolar concentration and that they recognise an epitope different from those of mAbs 7E11 and J591.

The stability of scFvD2B in different experimental conditions was investigated testing residual binding activity by ELISA/RIA. Incubation for 6 h in mouse sera and for 24 h in human sera, both potentially containing proteases, did not affect neither binding activity of scFvD2B (Fig. 4) nor its integrity, as assessed by SDS–PAGE (data not shown). Incubation of scFvD2B up to 48 h at 37 °C in complete medium or storage for 18 months at –20 °C indicated a good thermo-stability of the reagent (data not shown); furthermore, maintenance of function under acidic conditions was recorded.

#### 3.3. Internalisation of antigen–antibody complex

The evaluation was performed at 37 °C to activate the internalisation machinery and allow the PSMA-bound reagent to internalise; control samples were kept at 4 °C.

The internalisation of antibodies evaluated by immunofluorescence (Fig. 5A) indicated that a substantial amount of surface-bound anti-PSMA scFvD2B or IgGD2B was transferred to intracellular sites at 37 °C (left panel); in contrast, internalisation at 4 °C (right panels) was far less prominent as highlighted by the

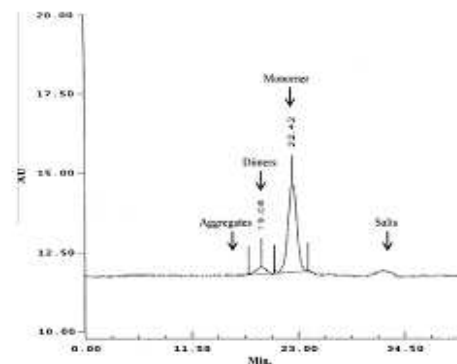


Fig. 1. Size exclusion chromatography of purified scFvD2B indicating a very low amount of dimers and the absence of aggregates.



## ARTICLE IN PRESS

B. Frigerio et al. / European Journal of Cancer xxx (2013) xxx–xxx

5

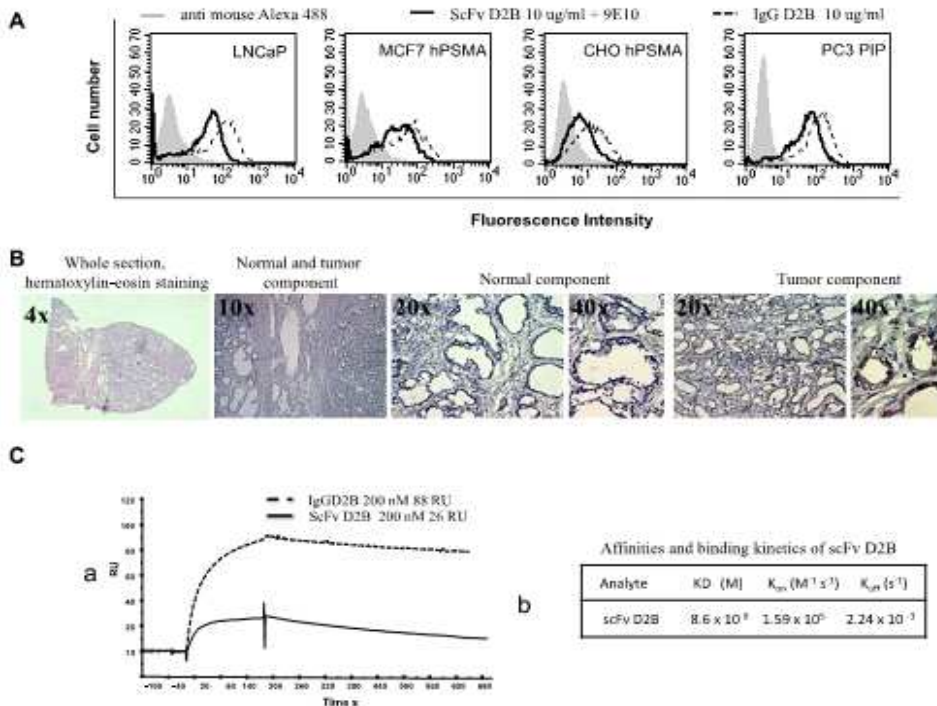


**Fig. 2.** (A) Flow cytometry: comparison of scFvD2B (solid line) binding to that of IgGD2B (dashed line) on prostate specific membrane antigen (PSMA) positive cell lines (no binding was observed on a PSMA negative cell line (data not shown)). The shift in fluorescence was assessed relative to a negative control (grey, cells incubated only with anti-mouse Alexa 488 or a control isotope matched mAb and anti-mouse Alexa 488). Approximately,  $5 \times 10^5$  cells were harvested, washed and incubated for 1 h on ice with scFvD2B (1 µg, 0.33 µM) or IgGD2B (1 µg, 67 nM) and diluted to 100 µL with phosphate buffered saline-bovine serum albumin (PBS-BSA) 0.05%. scFvD2B binding was detected using 9E10 followed by anti-mouse Alexa-488 antibody (Invitrogen), whereas that of IgGD2B was directly revealed by anti-mouse Alexa-488 antibody and analysed using a FACS-calibur and CellQuest software (Becton Dickinson, CA). (B) scFvD2B immunohistochemistry (IHC) reactivity of prostate carcinoma. Images on serial cryostat sections from left to right: haematoxylin-eosin stained sections (4×); scFvD2B immunohistochemical stain (10×) showing no reactivity on healthy component and positive reaction on tumour component in the same section; magnification 20× and 40× of normal component; magnification 20× and 40× of tumour component. (C) Biacore analysis: a standard amine-coupling protocol was used to immobilise on lane 2 the 7E11 antibody (40 µg/mL in  $CH_3COONa$  buffer 10 mM pH 4.8); lane 1 was used as a reference to subtract non-specific binding. LNCaP and PC3-PIP (0.5 mg/mL), or as a negative control IGROV-1 (0.5 mg/mL), lysates were injected three times at a flow rate of 30 µL/min for 10 min to enable the capture of soluble PSMA in the lysate by immobilised anti-PSMA 7E11. Human PSMA (hPSMA) from LNCaP lysate was captured on the sensorchip by the 7E11 mAb coupled as a ligand (360 RU) and 200 nM of scFvD2B or IgGD2B was injected for 3 min and then left for 15 min to follow dissociation; the binding observed in the sensorgram (a) with scFvD2B (26 RU) is only apparently lower than that observed with IgGD2B (88 RU) since its size is six times lower than that of the entire mAb. Affinity and kinetics of the interaction between PSMA and scFvD2B were determined by surface plasmon resonance measurements on LNCaP lysate (b); the same results were obtained with PC3-PIP lysate (data not shown). Kinetic analyses were performed in duplicate at concentrations ranging from 800 to 25 nM, but without glycine chip regeneration to avoid dissociation of soluble PSMA from 7E11. The restoration of initial baseline was verified after each injection.

amount of anti-PSMA reagents remaining at the cell surface.

The kinetics of PSMA internalisation mediated by the two  $^{111}In$ -reagents (Fig. 5B) were similar; after 5 min at 37 °C 20% to 60% of antigen-antibody complex

was internalised and, thereafter, the amount of internalised PSMA increased over time reaching a plateau in less than 2 h. When the internalisation triggering reagent was scFvD2B, the total amount of internalised complex was lower at each observation point but its monovalent

binding was able to internalise around 40% of the bound antigen in 2 h. Similar internalisation was recorded with <sup>131</sup>I-scFvD2B (data not shown).

3.4. Imaging *in vivo*

*In vivo* tumour detection capacity of either fluoro-chrome-labelled mAb or scFv was assessed by optical imaging in mice bearing established s.c. PC3 and PC3-PIP tumours (Fig. 6). Total body scanning disclosed that IgGD2B and derived scFvD2B presented different tumour detecting kinetics and biodistribution patterns. Indeed, the IgGD2B mAb initially produced a very diffuse signal from the entire body that also involved both tumours, irrespective of hPSMA expression, while a clear and specific accumulation in PC3-PIP was evident only after 24 h from injection. Conversely, scFvD2B showed high specificity and produced a detectable signal at the level of the hPSMA-expressing tumour only, with an emission peak at 3 h post-injection.

4. Discussion

Clinical management of prostate cancer requires accurate disease characterisation. Imaging is a promising diagnostic/prognostic tool and identification of sensitive and specific agents is one of the major goals for prostate cancer: mAbs represent ideal targeting agents. Towards this aim, PSMA has been targeted by several mAbs and some have already entered in clinical trials.<sup>21</sup> However, the recent demonstration, as in the case of CD20 and HER2,<sup>22</sup> that different antibodies targeting the same antigen, can differ widely from one another in terms of biological and clinical characteristics, as well as for their modes of action, justifies our attempt to develop new anti-PSMA mAbs.

In addition to specificity, other critical parameters for the successful *in vivo* use of antibodies in oncology are size, affinity, solubility and stability. Overall, poor *in vivo* distribution of intact mAbs, which reduces the penetration from vasculature into the solid tumour mass,<sup>23</sup>

and their prolonged residence in circulation, can lead to unacceptable background and side-effects when imaging or radioimmunotherapy is employed, thus limiting their application. On the contrary, antibody fragments, such as scFv, due to their small size can more easily penetrate into solid tumour masses and are cleared rapidly from the blood theoretically achieving much greater target specificity for tumour localisation.<sup>24</sup>

Furthermore, the entity of the human anti-mouse antibody (HAMA) response can be lessened by the use of antibody fragments lacking the Fc domain, in particular single-chain Fv antibody fragments (scFvs).<sup>25</sup> ScFvs, since they are not glycosylated, should be easily expressed in prokaryotic cells and produced at affordable costs. On these bases, we decided to develop a scFv starting from a new anti-PSMA candidate mAb, named D2B. scFvs are relatively unstable<sup>26</sup> and reported to form dimers and aggregates,<sup>27,28</sup> and, for protein therapeutics including mAbs, such aggregates can limit strongly *in vivo* applications since they may reduce the mAb efficacy and contribute to immunogenicity. Our biochemical data indicate that scFvD2B, even after radiolabelling, did not aggregate and that dimers are present in a very low amount (5–8%). In addition, probably due to a very stable pairing of the variable chains, scFvD2B could be produced on a laboratory scale with good yield, suggesting its successful production at larger scales. A sufficient resistance to serum proteases is essential for successful antibody *in vivo* applications and the possibility to expose them to harsh conditions, such as low pH, is an important screening parameter for selection of reagents suitable for diagnostic and therapeutic applications that require chemical manipulations. Thus, we investigated the stability of scFvD2B in serum and acidic conditions and after long storage, and in all cases we observed a good maintenance of functionality.

It has been reported that scFv in a format like that we generated, i.e. with a flexible peptide linker to covalently connect the VH and VL domains, can exhibit good antigen-binding activity compared to a non-disulphide-bonded Fv fragment. We demonstrated that scFvD2B,

Table 2  
Summary of scFvD2B and IgGD2B characteristics after radiolabelling with <sup>131</sup>I and <sup>111</sup>In.

Characteristics (%; mean ± SD)	<sup>131</sup> I-labelled reagents		<sup>111</sup> In-labelled reagents	
	scFvD2B (4–7 expts)	IgGD2B (2 expts)	scFvD2B (3–6expts)	IgGD2B (1 exp)
Efficiency	96.1 ± 1.4	92.0 ± 1.4	96.2 ± 0.9	99
Radiochemical purity	99.2 ± 0.6	97.5 ± 0.7	99.2 ± 0.4	99
Specific activity	2.4 ± 0.9	1.5 ± 0.7	1.8 ± 0.8	1.9
Immunoreactivity on PSMA <sup>+</sup> (prostate specific membrane antigen)cells				
LNCaP	68.0 ± 4.7	56.5 ± 2.1	52.7 ± 10.6	ND
PC3-PIP	71.3 ± 3.9	59.5 ± 2.1	63.8 ± 5.7	59
Immunoreactivity on PSMA <sup>-</sup> cells				
PC3	2.6 ± 0.9	1.9 ± 1.5	3.6 ± 1.6	1.9
A431	3.0 ± 0.2	ND	5.0 ± 1.7	ND

Please cite this article in press as: Frigerio B. et al., A single-chain fragment against prostate specific membrane antigen as a tool to build therapeutic reagents for prostate cancer, *Eur J Cancer* (2013), <http://dx.doi.org/10.1016/j.ejca.2013.01.024>

## ARTICLE IN PRESS

B. Frigerio et al. / European Journal of Cancer xxx (2013) xxx–xxx

7

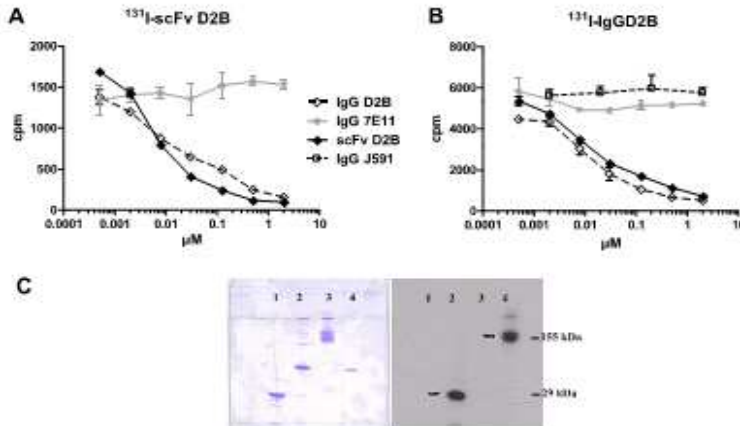


Fig. 3. Epitope identification by competition assay. Tracer amounts (20 nM) of  $^{125}\text{I}$ -scFvD2B (A) or  $^{125}\text{I}$ -IgGD2B (B) were mixed with titrated doses of unlabelled scFvD2B, IgGD2B, IgG7E11 or IgGJ591 (from 2  $\mu\text{M}$ ) and incubated for 3 h at 37 °C on PC3-PIP cells. (C) Integrity of scFvD2B before and after radiolabelling compared with IgGD2B. Left panel, sodium dodecyl sulphate–polyacrylamide gel electrophoresis (SDS–PAGE) loaded with 1  $\mu\text{g}$  of cold reagent scFvD2B (well 1) and IgGD2B (well 3) and with 40000 cpm of radiolabelled scFvD2B (well 2) and IgGD2B (well 4). Right panel, the same samples after autoradiography.

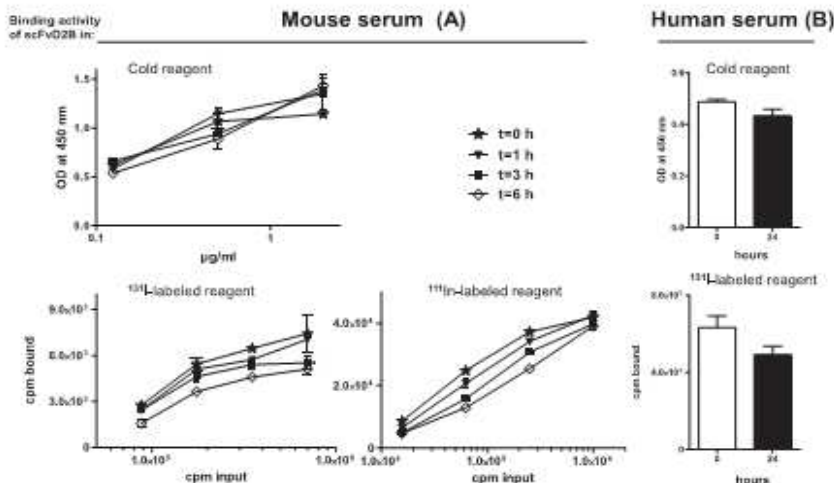


Fig. 4. Stability of scFvD2B in mouse (A) and human (B) serum at 37 °C, both unlabelled and after radiolabelling with  $^{125}\text{I}$  or  $^{111}\text{In}$ .

despite its monovalent binding, showed an affinity constant (KD) of 8.6 nM in BIAcore analysis, which is around 20 times lower than that of intact IgGD2B, but comparable to that of the entire IgG anti PSMA mAb J591 (1.8, 3 and 15 nM in three different reports,<sup>29–31</sup>), already entered in clinical use.<sup>32</sup> Moreover, the very slow dissociation constant from the

antigen argues for a high *in vivo* binding stability on the target. Our preliminary *in vivo* experiments using fluorescent label antibody demonstrate much more background for IgGD2B which seems to be distributed in an antigen-non-specific manner over many sites of the organism. This could mean that much of the initial mAb dose is retained by Fc-receptors on many cell types



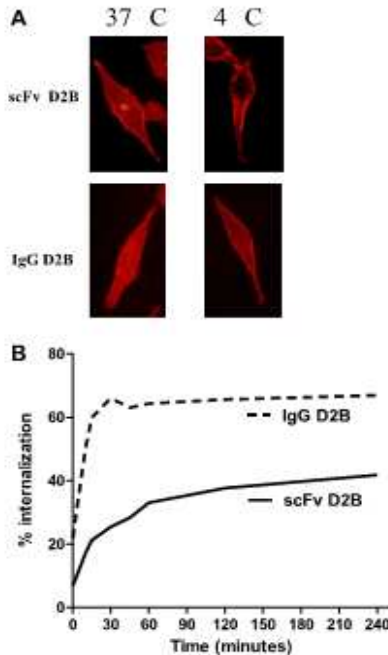


Fig. 5. Internalisation ability of scFvD2B and IgGD2B. (A) Fluorescent reagents incubated at 37 °C (left panel) and 4 °C (right panel). For immunofluorescence evaluation, cells grown on glass coverslips were incubated for 1 h with 1 µg of scFvD2B or IgGD2B. Cells were fixed and permeabilized with 7:2 acetone-methanol (v/v) for 10 min on ice and then incubated, for scFvD2B, with 9E10 followed by goat anti-mouse AlexaFluor 546, and for IgGD2B directly with the later reagent. (B) Internalisation ability of radiolabelled anti-prostate specific membrane antigen (PSMA) reagents. <sup>111</sup>In-labelled scFvD2B was incubated at 37 °C with PC3-PIP live cells and percentage internalisation evaluated after different lengths of incubation time. For radiolabelled experiments, cells cultured in 6-well Petri dishes to 80% confluence were incubated with <sup>111</sup>In- or <sup>113</sup>In-scFvD2B or -IgGD2B (20 nM) diluted in 1 mL of complete medium for different lengths of time (range 5 min–4 h). At each time point, after washing, cells were treated with 1 mL of glycine 100 mM, pH 2.8 and CH<sub>3</sub>COOH 100 mM for 20 min at room temperature to remove surface membrane-bound antibodies and supernatant was collected for radioactivity measurement. Subsequently, cells were lysed in 1 mL of NaOH 1 M for 20 min at room temperature and analysed for intracellular radioactivity. Radioactivity was determined using a COBRA II Auto-Gamma counter (Packard, Perkin Elmer, Boston, MA, USA). The percentage of internalisation was estimated as the ratio between the internalised and the total (internalised plus bound to membrane surface) radiolabelled antibody.

in the body. This leads to the loss of a large part of the initial dose by unspecific absorption through those receptors, which is not without systemic side-effects, whereas the use of scFvD2B, do not have this broad and diffuse effect. Moreover, to be able to use a scFv

for targeting, due to the rapid clearance, the strength of binding of the antibody fragment must be very high to permit to it to bind quickly and remain attached for a suitable length of time. Many studies have been performed to study the importance of the best format of antibodies and affinity indicating that reducing the circulation time the affinity must be improved to obtain productive results.<sup>33,34</sup> The high binding strength of our scFvD2B seems to be enough to have rapid localisation despite a very fast clearance.

Radiolabelling of scFvD2B was possible at very high efficiency suggesting that purification after labelling could be avoided making possible the development of a simple labelling kit accessible to all nuclear medicine facilities. The availability of radiolabelled reagents with high immunoreactivity allows the development of quantitative competition and internalisation assays. Competition data between IgGD2B and scFvD2B further indicated that the binding strengths of our two anti-PSMA reagents are quite similar. Furthermore, we confirmed that the anti-PSMA candidate mAb D2B, as well as its scFv, recognises a new epitope that is different from that of J591.

Other than antibody format, the target antigen characteristics as well as the fate of antigen-antibody complex after antibody binding are also important for the success of imaging and selection of therapeutic agents (radioisotopes, drugs and toxins). Despite its monovalent binding, the scFvD2B retained a good strength of binding and was able to internalise around 40% of bound antigen compared with the internalisation of the IgGD2B which is 60%. This observation would be consistent with the interpretation that crosslinking of two copies of PSMA by a bivalent binding mAb leads to a more potent internalisation than binding by a monovalent scFv.

All our *in vitro* data argued for a potential *in vivo* application of scFvD2B, while the experimental data documented its ability to specifically target only PSMA expressing prostate cancer xenografts.

In conclusion, our results clearly demonstrate that the PSMA-specific internalising scFvD2B, due to its advantageous properties, may be an ideal antibody fragment for the development of novel diagnostic/therapeutic methods to target imaging agents or for delivery of drugs for treatment of PSMA-positive tumours. The high stability of the molecule argues for further exploitation of scFvD2B to generate fusion proteins and build mono-specific multimeric or bi-specific reagents,<sup>35</sup> that upon preclinical validation, could hopefully enter into clinical use.

**Financial support**

We acknowledge Fondazione Monzino and Fondazione Cariplo to S.C., AIRC 5x1000 Bombardieri to M.F., AIRC 5x1000 2010 to A.R., e IG 13121 to A.R., Fondazione Cariverona (Verona Nanomedicine

## ARTICLE IN PRESS

B. Frigerio et al. / European Journal of Cancer xxx (2013) xxx–xxx

9

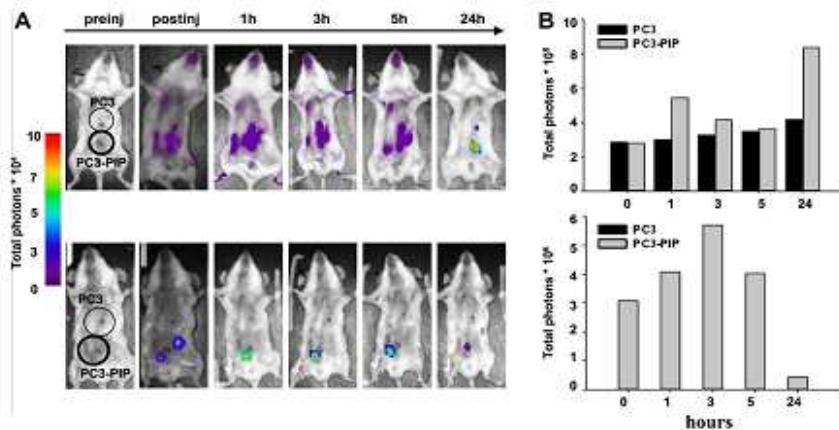


Fig. 6. Single-chain variable fragment (scFv) and IgGD2B mAb *in vivo* biodistribution. Mice bearing *s.c.* established PC3 and PC3-PIP tumours at two different sites were placed on a low manganese diet to reduce autofluorescence from normal mouse chow, and abdominal fur was removed by depilation. Three days later, animals were injected with 50  $\mu$ g of IgGD2B mAb (A, upper panels) or 50  $\mu$ g of scFvD2B (A, lower panels), and biodistribution kinetics of the compounds was assessed by fluorescence optical imaging as total body scanning with a 670 nm laser and a 693LP filter; the spatial resolution/scan step was fixed at 1.5 mm, exposure time was 0.5 s and laser power was automatically adjusted for each scan session. (B) Histograms report the relative total photons emitted from regions of interest around tumour sites from mice injected with IgGD2B mAb (upper panel) or derived scFvD2B (lower panel). Data are expressed as photon flux and quantified as photon  $s^{-1}$ . The figure shows one representative experiment of three that produced similar results.

Initiative and Interceptin Project) to M.C. and AIRC 5x1000 and Fondazione Cariverona/AIRC Progetto Regionale to M.C. for supporting this work.

#### Conflict of interest statement

None declared.

#### Acknowledgements

We would like to thank Dr. J. Benard (Gustave Roussy, Paris) and Dr. W. Heston (Department of Cancer Biology, Cleveland Clinic Main Campus) for providing the cell lines IGROV-1 and PC3-PIP, respectively; Dr. N.H. Bander (Medical College of Cornell University, New York) for supplying the mAb J951; Dr. Barbara Valeri of the Pathology Department for histopathologic examination; Dr. Silvia Veneroni and the Biorepository personnel of our Institute for valuable contribution in tissue sample collection; and Dr. Patrick Moore for editing of the manuscript.

#### References

- Israeli RS, Powell CT, Corr JG, Fair WR, Heston WD. Expression of the prostate-specific membrane antigen. *Cancer Res* 1994;54:1807–11.
- Wright GL, Haley C, Beckett ML, Schellhammer PF. Expression of prostate-specific membrane antigen in normal, benign, and malignant prostate tissue. *Urol Oncol* 1995;1:18–28.

- Wright Jr GL, Grob BM, Haley C, et al. Upregulation of prostate-specific membrane antigen after androgen-deprivation therapy. *Urology* 1996;48:326–34.
- Sweet SD, Pacelli A, Murphy GP, Bostwick DG. Prostate-specific membrane antigen expression is greatest in prostate adenocarcinoma and lymph node metastases. *Urology* 1998;52:637–40.
- Bouchelouche K, Choyke PL, Capala J. Prostate specific membrane antigen – a target for imaging and therapy with radionuclides. *Discov Med* 2010 Jan;9:55–61.
- Nelson AL, Dhimolea E, Reichert JM. Development trends for human monoclonal antibody therapeutics. *Nat Rev Drug Discov* 2010;9:767–74.
- Carter PJ. Potent antibody therapeutics by design. *Nat Rev Immunol* 2006;6:343–57.
- Ghosh A, Wang X, Klein E, Heston WD. Novel role of prostate-specific membrane antigen in suppressing prostate cancer invasiveness. *Cancer Res* 2005;65:727–31.
- Jachimowicz RD, Fracasso G, Yazaki PJ, et al. Induction of *in vitro* and *in vivo* NK cell cytotoxicity using high-avidity immunoligands targeting prostate-specific membrane antigen in prostate carcinoma. *Mol Cancer Ther* 2011;10:1036–45.
- Vellinga J, de VJ, Mybré S, et al. Efficient incorporation of a functional hypoxanthine-thymine-thymine single-chain antibody fragment protein-IX fusion in the adenovirus capsid. *Gene Ther* 2007;14:664–70.
- Lin H, Moy P, Kim S, et al. Monoclonal antibodies to the extracellular domain of prostate-specific membrane antigen also react with tumor vascular endothelium. *Cancer Res* 1997;57:3629–34.
- Hoogenboom HR, Griffiths AD, Johnson KS, et al. Multi-subunit proteins on the surface of filamentous phage: methodologies for displaying antibody (Fab) heavy and light chains. *Nucleic Acids Res* 1991;19:4133–7.
- Figini M, Obici L, Mezzanzanica D, et al. Panning phage antibody libraries on cells: isolation of human Fab fragments against ovarian carcinoma using guided selection. *Cancer Res* 1998;58:991–6.

14. Burastero SE, Frigerio B, Lopalco L, et al. Broad-spectrum inhibition of HIV-1 by a monoclonal antibody directed against a gp120-induced epitope of CD4. *PLoS One* 2011;6:e22081.
15. Robert R, Noubhani AM, Jacobin MJ, Santarelli X, Clouet-Sanchez G. Improvement in production and purification bioprocesses of bacterially expressed anti- $\alpha$ -hllb $\beta$ 5 human single-chain Fv antibodies. *J Chromatogr B Analyt Technol Biomed Life Sci* 2005;818:43–51.
16. Coliva A, Zacchetti A, Luison E, et al.  $^{90}\text{Y}$  labeling of monoclonal antibody MOv18 and preclinical validation for radioimmunotherapy of human ovarian carcinomas. *Cancer Immunol Immunother* 2005;54:1200–13.
17. Figini M, Martin F, Ferri R, et al. Conversion of murine antibodies to human antibodies and their optimization for ovarian cancer therapy targeted to the folate receptor. *Cancer Immunol Immunother* 2009;58:531–46.
18. Zacchetti A, Coliva A, Luison E, et al. (177)Lu-labeled MOv18 as compared to (131)I- or (90Y)-labeled MOv18 has the better therapeutic effect in eradication of alpha folate receptor-expressing tumor xenografts. *Nucl Med Biol* 2009;36:759–70.
19. Bobisse S, Rondina M, Merlo A, et al. Reprogramming T lymphocytes for melanoma adoptive immunotherapy by T-cell receptor gene transfer with lentiviral vectors. *Cancer Res* 2009;69:9385–94.
20. Martin ACR. Protein sequence analysis of antibody variable domains. In: Kontermann R, Dubel S, editors. *Antibody engineering*. 2001 ed. 2001. p. 423–439.
21. Olson WC, Heston WD, Rajasekaran AK. Clinical trials of cancer therapies targeting prostate-specific membrane antigen. *Rev Recent Clin Trials* 2007;2:182–90.
22. Shim H. One target, different effects: a comparison of distinct therapeutic antibodies against the same targets. *Exp Mol Med* 2011;43:539–49.
23. Jain RK, Baxter LT. Mechanisms of heterogeneous distribution of monoclonal antibodies and other macromolecules in tumors: significance of elevated interstitial pressure. *Cancer Res* 1988;48:7022–32.
24. Yokota T, Milevic DE, Whitlow M, Schlom J. Rapid tumor penetration of a single-chain Fv and comparison with other immunoglobulin forms. *Cancer Res* 1992;52:3403–8.
25. Goldenberg DM, Goldenberg H, Sharkey RM, et al. Clinical studies of cancer radioimmunodetection with carcinoembryonic antigen monoclonal antibody fragments labeled with  $^{125}\text{I}$  or  $^{99\text{m}}\text{Tc}$ . *Cancer Res* 1990;50:9096–21s.
26. Cheng LS, Liu AP, Yang JH, et al. Construction, expression and characterization of the engineered antibody against tumor surface antigen, p185(c-erbB-2). *Cell Res* 2003;13:35–48.
27. Arndt KM, Muller KM, Pluckthun A. Factors influencing the dimer to monomer transition of an antibody single-chain Fv fragment. *Biochemistry* 1998;37:12918–26.
28. Rothlisberger D, Honegger A, Pluckthun A. Domain interactions in the Fab fragment: a comparative evaluation of the single-chain Fv and Fab format engineered with variable domains of different stability. *J Mol Biol* 2005;347:773–89.
29. Smith-Jones PM, Vallababaisola S, Goldsmith SJ, et al. In vitro characterization of radiolabeled monoclonal antibodies specific for the extracellular domain of prostate-specific membrane antigen. *Cancer Res* 2000;60:5237–43.
30. McDevitt MR, Barendsward E, Ma D, et al. An alpha-particle emitting antibody ( $^{213}\text{Bi}$ J591) for radioimmunotherapy of prostate cancer. *Cancer Res* 2000;60:6095–100.
31. Fracasso G, Bellisola G, Cingarlini S, et al. Anti-tumor effects of toxins targeted to the prostate specific membrane antigen. *Prostate* 2002;53:9–23.
32. Akhtar NH, Pail O, Saran A, Tyrell L, Tagawa ST. Prostate-specific membrane antigen-based therapeutics. *Adv Urol* 2012;2012:973820.
33. Leyton JV, Olafsen T, Lepin EJ, et al. Humanized radiolabeled minibody for imaging of prostate stem cell antigen-expressing tumors. *Clin Cancer Res* 2008;14:7488–96.
34. Lepin EJ, Leyton JV, Zhou Y, et al. An affinity matured minibody for PET imaging of prostate stem cell antigen (PSCA)-expressing tumors. *Eur J Nucl Med Mol Imaging* 2010;37:1529–38.
35. Chan AC, Carter PJ. Therapeutic antibodies for autoimmunity and inflammation. *Nat Rev Immunol* 2010;10:301–16.

## **PART III**

**Creation of a completely human antibody fragment starting from the  
monoclonal antibody D2B.**

## Results and Discussion

### 1 Selection of human antibody fragments by panning with magnetic beads

The second part of my project is the creation of a completely human antibody fragment against PSMA. All the data obtained in the first part of my thesis demonstrate that scFvD2B have adequate functionality, specificity and binds, with good affinity, to an epitope different from those recognized by the other anti-PSMA antibodies commercially available. These characteristic make scFvD2B an ideal reagent for diagnostic and therapeutic practices. In order to reduce the potential immunogenicity of the reagent but maintain similar antigen-binding characteristics of the starting monoclonal antibody D2B, the guided selection procedure (also called epitope imprinting selection) has been used for the conversion of the murine antibody into completely human antibody fragments. This method uses a murine chain (in our case the light chain) to drive the selection of the other chain (in our case the VHCH). With this method, the murine variable domains are sequentially replaced by human variable domains. The antibody phage selection was performed on soluble PSMA after its immobilization using IgG anti-mouse beads for the binding of IgG7E11 that recognize the intracellular domain of PSMA. The first round of selection is the most important. Any errors made at this point will be amplified in subsequent rounds of selection.

It was calculated that after each round of selection there is a  $10^3$  fold enrichment of specific antibody. Ideally, only one cycle of selection should be required, but sometimes the binding of non-specific phages, due to their stickiness, limits their enrichment. For this reason 3-5 rounds of selection should be performed to select the desired antibody. In our cases three rounds of



selection were performed with different experimental conditions in order to select PSMA-specific phages. The hybrid polyclonal phages (composed by human VHCH1 and murine VKCK-D2B) recovered after each panning cycles were screened for binding by ELISA in order to identify "polyclonal" phage antibodies. ELISA was performed on PC3-PIP and PC3 cell lines. As shown in figure 14A there was an enrichment of binding capability with further rounds of selection and the binding is specific, in fact no binding was observed on PC3 cells (data not shown) indicating that the process was working.

Single clone phage ELISA was performed starting from randomly picked single colonies to identify positive "monoclonal" phage antibodies.

29 clones demonstrated ability to bind PC3-PIP and not the negative PC3 cell lines. Among those positive clones we identified two different heavy chains named VHCH-A and VHCH-B. The two corresponding genes were cloned into a vector containing a library of human light chains genes (VKCK). In this way the two human VHCH1 selected could drive the selection of a suitable human VKCK. Three panning cycles were performed as previous described. The polyclonal phages obtained after each panning were tested in ELISA but no evidence of binding improvement was found (Fig. 14B). Moreover from the single clone phage ELISA no clones with PSMA specificity were found (data not shown).

## **2 Binding of antibody fragments A and B**

To try to understand why we failed to select a suitable light chain we hypothesize that our VHCH could be able alone to bind the antigen and for that reason the VH selected are not able to drive selection of VL because not necessary. It is in fact described in literature [Harmsen and de Haard2007] that some antibody

chains alone are enough to bind the antigen and many groups started to study the so called single-domain antibodies or nanobodies demonstrating the functionality of VH alone.

Our failure in light chain selection could suggest that probably for some heavy chain the possible presence of a light chain could interfere with antigen binding. To confirm our hypothesis the two selected clones (clone A and clone B) have been built as VHCH1 or VH domain.

To determine whether VHCH-A and VHCH-B are specific for PSMA in absence of light chain, the antibody fragments were expressed on phage surface and tested in ELISA in comparison with the Fab format associated with the murine light chain. ELISA showed that hVHCHs have a higher binding than the respective Fabs (Fig. 15A) giving the proof that the heavy chain alone are able to bind the antigen and probably the presence of the light chain may decrease the strength of binding.

To verify whether soluble anti-PSMA hVHCHs retained the binding properties of the hVHCHs displayed on phages, soluble production of VHCH-A and VHCH-B were performed after cloning of the corresponding genes into a pUC vector. The periplasmic extract was analyzed in DOT-BLOT for production (Fig. 15B) and in ELISA to verify the functionality. No binding was observed on cells expressing PSMA (data not shown). A plausible interpretation of this observation is that when an antibody fragment is displayed on phage, it is more stable and/or it acquires a different conformation with a higher stability, which enhances its binding properties. Another explanation is that, phages may express more copies of the antibody fragments. This may increase the antibody valency with enhanced binding of the VHCH expressed on phage surface. Moreover the production in soluble form, as showed by DOT BLOT, indicates

a low yield of these fragments in the periplasm (at least for VHCH-B), which is probably not sufficient to see a binding.

### **3 VH-A and VH-B binding**

To investigate whether VHs domain are able to bind PSMA, the hVH genes were re-amplified with the appropriate primers and cloned into a phagemid vector that allow the production of both phages and soluble proteins. VH-A and VH-B expressed on phage surface were tested on ELISA and FACS analysis but no evidence of specific binding was observed (data not shown). The periplasmic extract of VH-A and VHB were produced, analyzed in DOT-BLOT to verify the production and in FACS to verify the functionality in soluble format. The result of the binding on PC3-PIP cells was negative. Because the DNA encoding the VHs was cloned into the pIT2 vector fused to a COOH-terminal hexahistidine sequence, recombinant VHs were purified by immobilized-metal affinity chromatography by using Ni-NTA agarose column. Purified VH-A and VH-B were tested on FACS analysis and a specific binding on PC3-PIP cell lines was observed (Fig.16) whereas no binding was observed on negative cells PC3 (data not shown). FACS analysis repeated after few days demonstrate a decreased binding indicating a problem in the stability of our fragments probably due to a formation of aggregates that is common for this kind of antibody fragments (Fig.16).

## 4 Mutagenesis

It is known that human heavy chains, that are naturally associated with the light chains, are less stable in its absence because the hydrophobic surface exposed confers to the antibody fragment a poor solubility and a tendency to aggregate. Nevertheless it is described that in addition to the conventional antibodies, camelids and sharks also produce unusual antibodies composed only of heavy chains lacking the light chain.

In order to improve the solubility of our antibody fragments we decided to compare the differences between the heavy chains produced by camelids, that were evolved naturally lacking a light chain, and our heavy chains. By comparative analysis with VHH domains of Camelidae we found that some aminoacidic residues that are normally involved in binding with light chain, in camelids are different than in humans conferring more hydrophilicity to the molecule. The residues Val37, Gly44, Leu45, and Trp47 are all conserved in human VH framework 2 and seems to be involved in interdomain contacts; these amino acid residues in original VHH domains of Camelidae, are substituted by hydrophilic residues Phe37, Glu44, Arg45 and Gly47. Therefore, to mimic the VHH of Camelidae, single and multiple amino acid substitutions were introduced into VHCH-A and VHCH-B using the QUIKCHANGE XL SITE-DIRECTED MUTAGENESIS KIT (Stratagene). We constructed a set of three mutants for each clone with gradual increasing “camelization”. In mutant A/37 the Val37 residue in VHCH-A framework 2 was substituted by Phe37. In mutant A/44, Gly44, Leu45 and Trp47 in framework 2 were substituted by Glu44, Arg45 and Gly47, respectively. In mutant A/D, the four mutations described above (V37F, G44E, L45R and W47G) were all introduced into the VHCH-A. The same mutations were introduced in VHCH-B (called B/37-

B/44- B/D). All six mutants were expressed in the periplasm, the yields of soluble mutated clones were similar of the non mutated clones (data not shown) and all modifications of the VHCHs showed a weak effect on the stability (data not shown), reduced specific binding to PC3-PIP and increased non specific binding on PC3 cells as showed in figure 17. At this point of the research we evaluated the possibility to introduce more mutations to stabilize the antibody fragments, in fact in literature are described other residues that could be modified to improve the stability of human VHCH1 including also the insertion of 2 cysteins at the positions 22 and 92 that allows the formation of an intradomain disulfide bridge. But, as our goal was to produce a human antibody fragment, in order to obtain a reagent less immunogenic as possible we decided to avoid further modifications residues that could potentially increase the immunogenicity.

## Conclusion and Future Prospects

The results obtained in this part of the project demonstrate that the isolated human VHs are able to bind PSMA in native form but that they are not stable. More stability studies need to be performed in order to obtain a suitable reagent with desirable properties for biopharmaceutical development.

To this aim we will proceed into two directions:

A) stabilization of the already isolated VH;

B) selection of new fragments using different methods.

A) Two approaches are under evaluation: first, a company called GlyTec, Inc has been contacted that will study the possibility to stabilize the two VH selected using different human oligosaccharides; second, in nature are described some light chains called “universal light chains” associated to heavy chains but not involved in the binding with the antigen as demonstrated by their high similarity to the germline sequence. We plan to associate this human light chain to our VHs and evaluate if this is sufficient to stabilize our molecules.

B) In order to overcome the selection of antibody fragments prone to aggregate, the strategy that will be performed was first described by Greg Winter group [Jespers *et al.* 2004] and it is based on heat denaturation of the library expressing the antibody fragment followed by panning and selection as usual in order to select in origin more stable antibody fragments.

## Figures

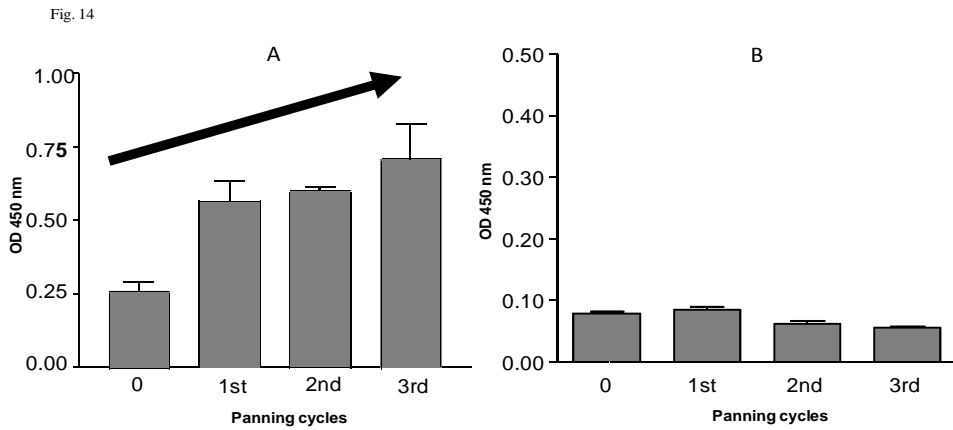


**Fig. 14.** Polyclonal Phage ELISA. Binding of original library, 1°, 2° and 3° round of selection phages composed by human VHCH associated to murine VLCL (A) and by human VHCH associated to human VKCK (B).

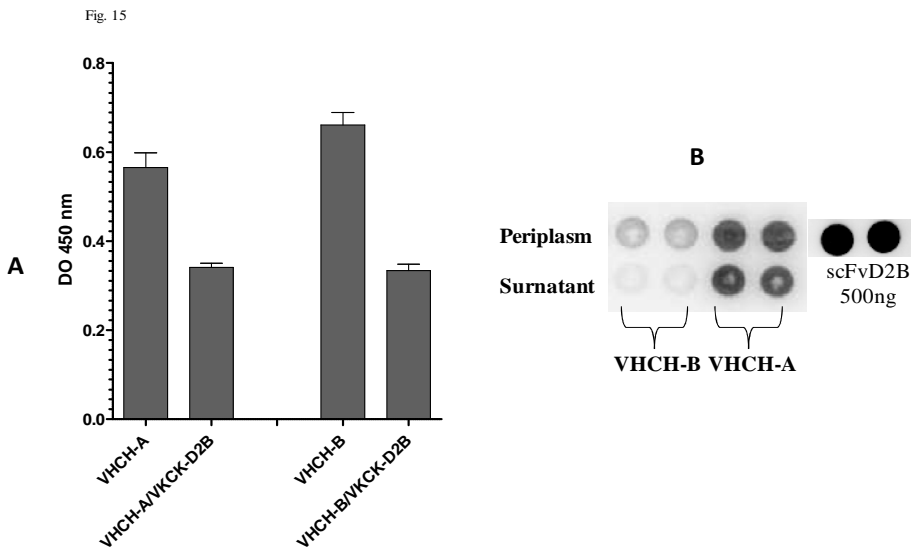


**Fig. 15.** A) ELISA assay. Binding comparison between phages expressing only VHCH-A or -B versus phages expressing VHCH-A or -B associated with murine VKCK D2B. B) DOT BLOT analysis. Evaluation of production in bacteria periplasm or in surnatant culture of soluble VHCH-A and soluble VHCH-B

Fig. 16

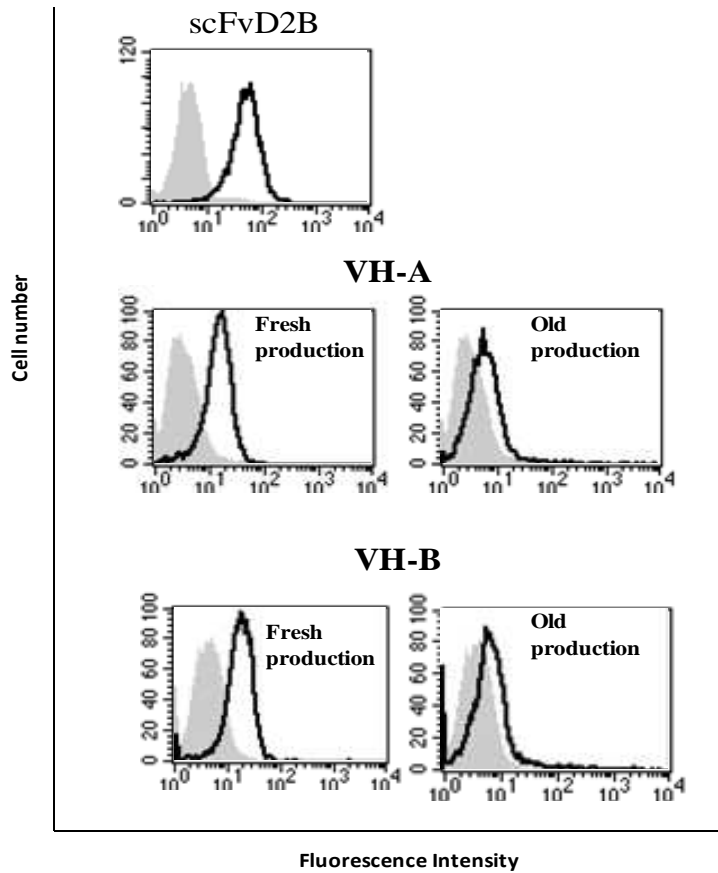


**Fig. 16.** FACS analysis. Binding comparison between soluble VH-A and VH-B tested immediately after production (fresh production) and after one week (old production). The shift in fluorescence was assessed relative to a negative control (gray).



Fig. 17

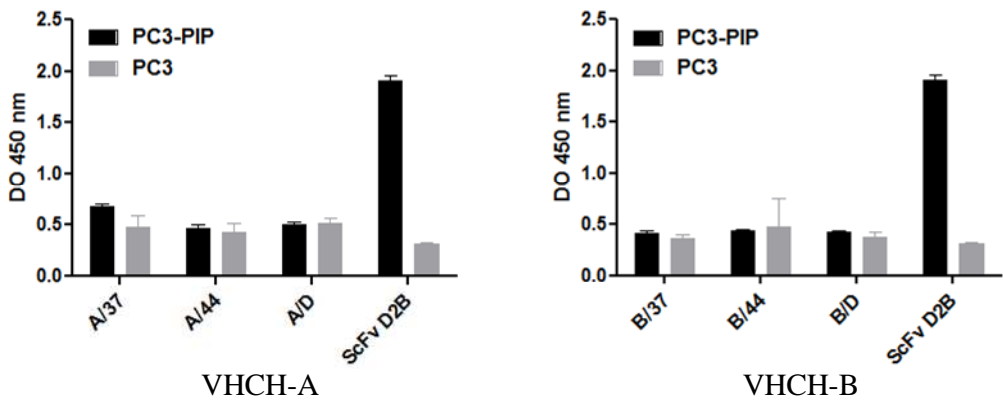


**Fig. 17.** ELISA assay. Binding of soluble VHCH-A and VHCH-B after the introduction of mutations.